Science
AAAS

Supplementary Materials for

Fumarate is a terminal electron acceptor in the mammalian electron transport chain

Jessica B. Spinelli *et al.*

Corresponding author: Jessica B. Spinelli, spinelli@wi.mit.edu

Science **374**, 1227 (2021)
DOI: 10.1126/science.abi7495

The PDF file includes:

Other Supplementary Material for this manuscript includes the following:

Materials and Methods

Cell Culture: The 143B osteosarcoma cell line, C2C12 mouse myoblast cell line, SW1353 chondrosarcoma cell line, DLD1 colon adenocarcinoma cell line, HCT116 colorectal carcinoma cell line, and U87 glioblastoma cell line were cultured in Dulbecco's Modified Eagle Medium (DMEM) (ThermoFisher) supplemented with 5% Heat Inactivated Fetal Bovine Serum (ThermoFisher) and 1% penicillin and streptomycin (ThermoFisher), and 0.1 mg/mL uridine (Sigma). The MINK Lung cell line and ATCC Fibroblast cell line were cultured in Fibroblast Basal Medium (Fischer Scientific) supplemented with the components of the low serum Fibroblast Growth Kit (Fischer Scientific). For experiments that required culturing cells in hypoxia, medium was pre-adapted in a hypoxia incubator (Baker Ruskinn) set to the appropriate oxygen level for at least 24 hours. For experiments involving expression of the alternative oxidase (AOX) or the class 1 DHODH, cells in all genetic conditions were treated with 100 ng/mL doxycycline (Takara Bio) for 24 hours to induce its expression. Inhibitors and other supplements: 100 nM – 2 μM antimycin (Thermo Fisher Scientific), 5 mM pyruvate (Sigma), 10-20 mM Aspartate (Sigma), 2 μM brequinar (Sigma), 1 μM Rotenone (Sigma), 1 μM – 5 μM piericidin (VWR), 10-20 mM Malonic Acid (Sigma), 500 nM Tetramethylrhodamine, Ethyl Ester, Perchlorate (TMRE) (ThermoFisher), 250-500 nM Carbonyl cyanide 3-chlorophenylhydrazone (Sigma). Cells were periodically tested for mycoplasma (SouthernBiotech).

Proliferation: 25,000 cells were seeded in 6-well dishes and counted on day 1 and day 5 on a Beckman Coulter Counter. Doubling times were calculated using the following equation:

Doublings = LN(2)/(LN(Day 5 Count/ Day 1 Count))

Generation of Stable Cell Lines: Single Guide RNAs (sgRNAs) against SDHA (ACCGTGCATTATAACATGGG), SDHB (TCCTTTATCACATACATGTG), UQCRC2 (TAAAGCAGGCAGTAGATATG), COX4 (GAACTTAATGCGATACACTG), were subcloned into the plentiCRISPR V1 (Addgene 52963). Subcloned plasmids were co-transfected into HEK293T cells with lentiviral packaging vectors. 143B cells were subsequently infected with the lentivirus and selected with puromycin, generating stable knockout cell lines. Single cells were sorted on a FACS Aria (BD Biosciences) to isolate clones. Clones were cultured and screened for the relevant knockouts. cDNA rescue experiments were performed by expressing cDNAs harboring silent mutations, rendering them resistant to sgRNAs in the knockout cells. cDNAs were cloned into pCW57.1 N-term GFP tTA (Addgene 107551) and stably expressed in knockout cells. Alternative Oxidase cDNA and the class 1 DHODH cDNA were cloned into a pCW57.1-Luciferase backbone (Addgene 9928). All plasmids were sequence verified (Quintara Biosciences) and will be available on Addgene.

Western Blots: Adherent cells were lysed in RIPA buffer (150 mM NaCl, 50 mM Tris-HCl, pH 7.5, 0.1% SDS, 1% Triton-X 100 (Sigma), 0.5% deoxycholate (Sigma), cOmplete EDTA-free protease inhibitor (Sigma)) and clarified by centrifugation. Protein content was quantified using a Pierce BCA Protein Assay Kit (Life Technologies) and 30-50 μg protein were loaded on 12% Tris-Glycine Novex Gels (Invitrogen). Proteins were subsequently transferred to a 0.45 μm PVDF membrane (Sigma). Primary antibodies were used at the following dilutions in 5% BSA: SDHA (Proteintech; 1:1000), NDUFV1 (Abcam; 1:1000), Total OXPHOS Rodent WB Antibody Cocktail- containing UQCRC2, SDHB, and ATP5A (Abcam; 1:1000), COX IV (Cell Signaling

Technology; 1:1000), MT-ND5 (Abcam; 1:1000), FLAG (Sigma; 1:1000), HIF1a (Cell Signaling Technology; 1:1000), ATP citrate lyase (Abcam; 1:1000), Citrate Synthase (Cell Signaling; 1:1000). Secondary antibodies were used at the following dilutions in 5% Milk: Anti-rabbit IgG HRP-linked Antibody (1:5000, Cell Signaling Technology), Anti- mouse IgG HRP-linked Antibody (1:5000, Cell Signaling Technology). Blots were developed using SignalFire ECL Reagent (Cell Signaling Technology) and exposed to autoradiography film.

Isolation of Mitochondria for Biochemical Assays: 143B cells were scraped and pelleted at 1000 x g for 5 minutes. Cell pellets were washed in 1X PBS and pelleted at 1000 x g for 5 minutes. For tissue samples, approximately 100 mg of tissue was weighed out. Tissue was powderized under liquid nitrogen with a mortar and pestle. Tissue powder or cells were re-suspended in isolation buffer (200 mM sucrose, 10 mM Tris HCl, 1 mM EGTA/Tris, pH 7.4 (adjusted with 1M HEPES)), transferred into an ice-cold glass homogenizer (VWR), and dounced with 15-30 strokes. Homogenates were transferred into tubes and centrifuged at 600 x g for 10 minutes at 4^{o}C. Supernatants were moved to a new tube and centrifugation was repeated. Then, supernatants were moved to a new tube and pelleted at 7,000 x g for 10 minutes at 4^{o}C. Pellets were washed in isolation buffer and centrifugation was repeated. Pellets were subsequently stored at -80^{o} C until use.

Blue Native Gel: Blue Native PAGE gels were run as previously described (60). Mitochondria were isolated as described above. 50 μg of mitochondrial protein was re-suspended in sample buffer cocktail containing 1X Native PAGE Sample Buffer (Life Technologies) and 8g digitonin /g mitochondrial protein. Samples were incubated on ice for 20 minutes and then centrifuged at 20,000 x g for 10 minutes at 4^{o}C. Coomassie G-250 sample additive (Life Technologies) was combined to 1/4th the final protein concentration in the supernatant. Samples were loaded onto NativePAGE 3-12% Bis-Tris Protein Gels (Life Technologies) and initially run in dark blue cathode buffer (1X Native PAGE anode buffer (Life Technologies), 0.2 mg/mL G-250 sample additive (Life Technologies)) for 30 minutes and subsequently switched to light blue cathode buffer (1:10 dilution of dark blue cathode buffer in 1X Native PAGE anode buffer (Life technologies)) for an additional 150 minutes. Gels were transferred onto a 0.45 μm PVDF membrane (Sigma) using 1X NuPAGE Transfer Buffer (Life Technologies) supplemented with 10% methanol. Membranes were subsequently washed with 8% acetic acid followed by 100% methanol and probed for relevant proteins using the western blot protocol described above (61).

Complex 1 activity assay (DCPIP): Purified mitochondria were re-suspended in buffer (0.22 M Mannitol, 0.075 M Sucrose, 1 mM EDTA, 10 mM HEPES pH 7.4, and one cOmplete Protease inhibitor tablet (Sigma)) to a concentration of 5 mg/mL. Mitochondria underwent 5 freeze-thaw cycles to permeabilize them. 50 μg of mitochondrial protein was used for each reaction and mixed with complex 1 activity assay buffer (25 mM KH_2PO_4 pH 7.5, 1 μM decylubiquinone (Sigma), 300 μM 2,6-dichlorophenolindophenol (VWR), 3.5 g/L BSA) supplemented with 10 μM antimycin (Sigma). Either 1 μM rotenone or equivalent DMSO was added to each well and baseline absorbance at 600 nm was measured on a SpectraMax iD5 plate reader (Molecular Devices). Reactions were initiated by adding NADH (Sigma) to a final concentration of 2 mM and absorbance at 600 nm was monitored over time.

DHODH activity assay: Assay was performed as previously described (62). Briefly, 1 X 10^6 143B cells were seeded 24 hours prior to the assay. Cells were pelleted, resuspended in 1 mL of

KPBS (136 mM KCl (Sigma), 10 mM KH_2PO_4 (Sigma) (pH 7.25)), and permeabilized using 5 freeze-thaw cycles. 280 µL of lysate was incubated with 20 µL of 20 mM dihydroorotate (Sigma) and 700 µL of DHODH activity buffer (500 µM dihydroorotate, 200 mM K_2CO_3-HCl (pH 8.0), 0.4% Triton X-100 (Sigma), 78 µM decylubiquinone (Sigma)) at 37°C at 850 rpm in a ThermoMixer (Eppendorf) for 30 minutes. Then, 100 µL of this mixture was incubated with 150 µL of Milli-Q water, 250 µL of 80 mM K_2CO_3 (Sigma), 250 µL of 8.0 mM $K_3[Fe(CN)_6]$ (Sigma), and 250 µL of 8.0 mM 4-TFMBAO (Sigma) at 95°C for 5 minutes. After quenching the reaction in an ice-water bath for 2 minutes, the fluorescence was read in a black Costar 96-well plate with a clear bottom using a SpectraMax iD5 at excitation and emission wavelengths of 320 nm and 420 nm, respectively. Orotate production was quantified using a standard curve in the range of 0 – 10 mM orotate.

SDH Activity Assay: Purified mitochondria were re-suspended in buffer (0.22 M Mannitol, 0.075 M Sucrose, 1 mM EDTA, 10 mM HEPES pH 7.4, and one cOmplete Protease inhibitor tablet (Sigma)) to a concentration of 5 mg/mL and underwent 5 freeze-thaw cycles to permeabilize them. 30 µg mitochondria (6 uL) were diluted 1:10 (in 54 uL) of SDH activity assay buffer (27.5 mM KH_2PO_4 pH 7.4, 1.1 mM CoQ-10 (Sigma), 3.5 g/L BSA). Reactions were supplemented with DMSO, 1 µM antimycin, or 1 µM piericidin and pre-incubated at 37 ºC for 10 minutes. Fumarate reduction reactions were initiated by adding NADH to a final concentration of 1 mM and fumarate to a final concentration of 10 mM. Succinate oxidation reactions were initiated by adding succinate to a final concentration of 10 mM. Reactions were quenched at the appropriate timepoints with 80% methanol:20% Water and vortexed for 10 minutes at 4 ºC. Samples were centrifuged at 16,000 x g for 10 minutes at 4 ºC and supernatants were dried down and analyzed by LC-MS for succinate and fumarate.

Oxygen Consumption Rate (Seahorse): Respiration was measured on intact 143B cells and on mitochondria purified from tissue on the Seahorse XFe-96 Analyzer (Seahorse Bioscience). Cells were incubated in a non-CO_2 37 ºC incubator in serum-free Seahorse XF RPMI Media (Seahorse Bioscience, Catalog # 103336) supplemented with 5 mM glucose, 2 mM glutamine, and 1 mM pyruvate. Oxygen consumption rate (OCR) was measured over a period of 30 minutes. Oxygen consumption rate was also measured on mitochondria purified from mouse tissues. Mitochondria were incubated in MAS buffer (70 mM sucrose, 220 mM mannitol, 10 mM KH_2PO_4, 5 mM $MgCl_2$, 2 mM HEPES pH 7.2, 1 mM EGTA, 2% BSA) supplemented with 2 mM ADP, 5 mM glutamate, 5 mM malate, 5 mM pyruvate, and 2.5 mM succinate. Oxygen consumption rate (OCR) was measured over a period of 30 minutes.

Oxygen Consumption Rate (Resipher): 25,000 143B cells were seeded into Thermo Nunc Treated, Flat-Bottom 96-Well Microplate (167008) in standard culture medium 24 hours prior to experimentation. On the day of experimentation, medium was changed and the Resipher oxygen sensing lid (Lucid Scientific) was attached. Live oxygen consumption rate was measured for 3 hours and then medium was changed to treat cells with the appropriate inhibitors. Live oxygen consumption rate was monitored for an additional 3 hours. Data were analyzed on Resipher web application (Lucid Scientific).

MT-DNA Quantification: Cells were pelleted, washed 1X in PBS, and then lysed in buffer (25 mM NaOH, 0.2 mM EDTA) for 15 minutes at 95 ºC. Lysis was neutralized with buffer (40 mM Tris-HCl) and centrifuged at 16,000 x g for 10 minutes at 4 ºC. Supernatant containing

MT-DNA was quantified on a CFX96 Real-Time System Thermal Cycler (Bio Rad). Primers amplifying the MT-DNA marker D-Loop (Forward Primer-tatcttttggcggtatgcacttttaacag Reverse Primer- tgatgagattagtagtatgggagtgg) and the nuclear DNA marker β-Globin (Forward Primer- gtgcacctgactcctgaggaga Reverse Primer- ccttgataccaacctgcccag) were used and the relative MT-DNA to nuclear DNA was quantified in each sample (63).

Immunofluorescence assays: 143B cells were seeded onto cover slips at 50% density for 24 hours and then fixed with 4% paraformaldehyde for 15 minutes. Then, cells were permeabilized in 0.25% Triton X-100 in PBS for 5 minutes, followed by blocking in CST blocking buffer (5% Donkey Serum (Sigma), 0.3% Triton X-100) for 30 minutes and incubated for 1 hour with primary antibodies against COX4 (Cell Signaling Technology) or FLAG (Cell Signaling Technology) at 1:200 diluted in buffer (1% BSA, 0.3% Triton X-100 in PBS). Secondary antibodies 568 Donkey anti-rabbit (Invitrogen) and 488 Donkey-anti-mouse (Invitrogen) were diluted to 1:500 in buffer (1% BSA, 0.3% Triton X-100 in PBS) and incubated for an hour at room temperature. Cover slips were mounted using ProLong Gold + DAPI (ThermoFisher) and imaged on a confocal microscope (Zeiss).

Live Cell Imaging: 143B cells were seeded at 50% density in 6-well dishes 24 hours prior to the experiment. Cells were pre-incubated with 500 nM TMRE dye for 30 minutes and then imaging on a Nikon TE2000 inverted microscope was started. Images were taken at 1 minute intervals over the course of an hour in the mCherry channel while the plate was incubated in a chamber maintaining a temperature of 37 ^{o}C and 5% CO_2.

Flow Cytometry: Cells were seeded 24 hours prior to the experiment at 50% density. On the day of the experiment, the cells were treated for the designated time with inhibitors. 30 minutes prior to the end of the incubation, 500 nM TMRE dye was added to the wells. Following incubation cells were washed, trypsinized, and filtered through a cell strainer prior to sorting. Fluorescence-activated cell sorting was performed on a LSR-II sorter, in which the fluorescence intensity of individual cells was quantified in the PE channel. Data were analyzed using FlowJo software (TreeStar).

Mouse Experiments: All mouse protocols were approved by the Institutional Animal Care and Use Committee (IACUC) at Massachusetts Institute of Technology. Wild-type C57BL/6J mice acquired from The Jackson Laboratory were housed in the Whitehead Institute Animal Facility and maintained according to the Sabatini Lab protocol approved by the Committee on Animal Care (0718-065-21). *In vivo* stable isotope tracing experiments were performed by retro-orbital and intraperitoneal bolus injections of $^{13}C_5{}^{15}N_2$-glutamine (50 mg/mL) dissolved in Hank's Balanced Salt Solution (Sigma), 200 μL in each injection site of 12-16 week old male and female wild-type C57BL/6J mice (Jackson Laboratory). Mice were euthanized 20 minutes after the injections. Tissue were harvested, flash frozen in liquid nitrogen, and stored at -80 ^{o}C until samples were ready for processing.

Exercise on treadmill: 12-week-old female mice were acclimated to a motorized treadmill (TSE systems, incline 5°) for two days prior to the forced running protocol. Mice were trained at 0.17 m/sec on each of the two training days for 20 minutes. On the day of running, mice were subjected to the following running protocol: 0.17 m/sec for 40 min, 0.18 m/sec for 10 min, 0.2 m/sec for 10 min, 0.22 m/sec for 10 min, 0.22-0.25 m/sec for 10 min, 0.25-0.28 m/sec for 10 min, 0.28-0.31 m/sec for 10 min and 0.31-0.32 m/sec for 5 min (Exhausted group). The 30 min

group was only subjected to 0.17 m/sec for 30 min. All mice were injected with $^{13}C_5{}^{15}N_2$-glutamine (50 mg/mL), 200 μL intraperitoneal and 50 μL intramuscular, and placed back on the treadmill (Exhausted and 30 min group) or in the cage (Rested group) 15 min before organs were harvested. Organs were harvested and snap frozen immediately after taking the mice off the treadmill.

Metabolite profiling:

A. Stable isotope tracing in cells: Cells were seeded 24 hours prior to the experiment in 6-well dishes at 70% density. For stable isotope tracing of glutamine, glutamine-free DMEM (ThermoFisher) was supplemented with 2 mM $^{13}C_5{}^{15}N_2$-glutamine (Sigma), 1 mM pyruvate, 5% FBS, 1% P/S, 0.1 mg/mL uridine. For stable isotope tracing of aspartate, DMEM containing 5% FBS , and 1% penicillin and streptomycin, and 0.1 mg/mL uridine (Sigma) was supplemented with the designated amount of $^{13}C_4$-aspartate (Sigma) and the pH adjusted to 7.4. uridine was left out of the medium for stable isotope tracing experiments measuring nucleotide biosynthesis. Unless otherwise stated, for all experiments, cells were treated for 8 hours and metabolites were isolated as described below. Relevant compounds were added at the start of the incubation periods.

B. *Ex vivo* stable isotope tracing on tissues: Tissues were excised from mice and washed in 1X PBS. Tissues were then cut into small pieces and placed in the appropriate stable isotope tracing medium. Stable isotope tracing medium contained either $^{13}C_5{}^{15}N_2$-glutamine (Sigma) or $^{13}C_4$-aspartate (Sigma) dissolved in DMEM, 5% FBS, 1% P/S. For *ex vivo* tracing experiments performed on the brain, the same medium was used without FBS. Tissues were incubated for the designated time at 37 ^{o}C in a normal or hypoxia tissue culture incubator. Tissues were removed from the medium, washed with PBS, and flash frozen in liquid nitrogen. Samples could be stored at -80 ^{o}C until metabolites were isolated.

C. Isolation of metabolites from adherent cells: To isolate metabolites, medium was removed, cells were washed 2 times with ice cold 1X PBS, and wells were covered in LC-MS grade 80:20 methanol:Water (ThermoFisher). Plates were scraped on dry ice and lysates were collected into Eppendorf tubes. Lysates were vortexed for 10 minutes at 4 ^{o}C and centrifuged at 16,000 x g for 10 minutes at 4 ^{o}C. Supernatants were immediately dried down in a Refrigerated CentriVap Benchtop Vacuum Concentrator connected to a CentriVap-105 Cold Trap (Labconco). Dried pellets were stored at -80 ^{o}C until they were run on LC-MS.

D. Isolation of metabolites from tissues: Tissues were flash frozen and powderized with a mortar and pestle in a liquid nitrogen bath. Approximately 30 mg of tissue powder was transferred into Eppendorf tubes and re-suspended in 800 uL ice-cold LC-MS grade 60:40 methanol:Water (ThermoFisher). Samples were vortexed for 10 minutes at 4 ^{o}C. Then, 500 uL of ice-cold LC-MS grade chloroform (ThermoFisher) was added to the lysate and samples were vortexed for an additional 10 minutes at 4 ^{o}C. Samples were centrifuged at 16,000 x g for 10 minutes at 4 ^{o}C, creating three layers: the top layer containing polar metabolites, the bottom layer containing non-polar metabolites, and the middle layer containing protein. The top layer was transferred to a new tube, dried down in a speedvac, and subsequently stored at -80 ^{o}C until they were analyzed by LC-MS. The

protein layer was separated from the non-polar layer and re-suspended in RIPA buffer (150 mM NaCl, 50 mM Tris HCl pH 7.5, 0.1% SDS, 1% Triton-X 100 (Sigma), 0.5% deoxycholate (Sigma), cOmplete EDTA-free protease inhibitor (Sigma)) to isolate protein. Protein in each sample was quantified using the Pierce BCA Protein Assay Kit (Life Technologies). Protein concentrations were used for normalization of sample inputs prior to LC-MS analysis.

E. Sample prep for LC-MS: Metabolite pellets were re-suspended in LC-MS grade water (ThermoFisher) and vortexed for 10 minutes at 4 ^{o}C. Samples were centrifuged at 16,000 x g for 10 minutes at 4 ^{o}C and supernatant was moved into LC-MS vials.

F. Liquid Chromatography and Mass Spectrometry (polar): A QExactive bench top orbitrap mass spectrometer equipped with an Ion Max source and a HESI II probe coupled to a Dionex UltiMate 3000 HPLC system (Thermo Fisher Scientific) was used to perform all LC-MS experiments. The instrument underwent mass calibration using the standard calibration mixture every 7 days. 2 uL of re-suspended polar metabolite samples were injected onto a SeQuant ZIC-pHILIC 5µm 150 x 2.1 mm analytical column equipped with a 2.1 x 20 mm guard column (MilliporeSigma). The column oven was held at 25°C and the autosampler tray was held at 4°C. Buffer A was comprised of 20 mM ammonium carbonate, 0.1% ammonium hydroxide. Buffer B was comprised of 100% acetonitrile. The chromatographic gradient was run at a flow rate of 0.150 mL/min as follows: 0-20 min: linear gradient from 80-20% B; 20-20.5 min: linear gradient from 20-80% B; 20.5-28 min: hold at 80% B. The mass spectrometer was operated in full-scan, polarity-switching mode, with the spray voltage set to 3.0 kV, the heated capillary at 275°C, and the HESI probe at 350°C. The sheath gas flow was 40 units, the auxiliary gas flow was 15 units, and the sweep gas flow was 1 unit. MS data was collected in a range of m/z = 70–1000. The resolution set at 70,000, the AGC target at $1x10^{6}$, and the maximum injection time at 20 msec. An additional scan (m/z = 220-700) was included in negative mode only to enhance detection of nucleotides.

G. Ubiquinone and Ubiquinol measurements: Ubiquinone and Ubiquinol were isolated from mitochondria purified by differential centrifugation as described above. Extraction and mass spectrometry protocols were performed with slight modifications to a previously described protocol (64). Briefly, mitochondria isolated from 25 million cells or approximately 100 mg mouse tissue were resuspended in 500 µL of ethanol and vortexed for 10 minutes at 4°C. Then, 1 mL of hexane was added and the samples were vortexed for an additional 10 minutes at 4°C. Samples were centrifuged at 16,000 x g for 10 minutes at 4 ^{o}C, creating two layers – the top hexane layer and bottom ethanol layer. The top (hexane) fraction was moved into a new tube and dried down. Immediately prior to LC-MS, samples were resuspended in 50 µL of 80:20 ethanol:hexane and loaded into a 4 ^{o}C autosampler. 5 uL of samples were injected onto a Luna 3 µm PFP(2) 100 Å, LC Column 100 x 2 mm. The column oven was held at 25°C and the autosampler tray was held at 4°C. Buffer A contained water with 0.1% formic acid and Buffer B contained acetonitrile with 0.1% formic acid. The gradient was as follows: 0 to 3 min, hold at 30% A, 3 to 3.25 min, gradient to 2% Buffer A, 3.25 to 5 min, hold at 2% Buffer A, 5 to 6 min, gradient to 1% Buffer A, 6 to 8.75 min, hold at 1% Buffer A, 8.75 to 9 min, gradient to 30% Buffer A and 9 to 10 min, hold 30% Buffer A. The chromatographic

gradient was run at a flow rate of 0.50 mL/min. The mass spectrometer was operated in full scan, positive-ion mode, with the spray voltage set to 3.0 kV, the heated capillary at 275°C, and the HESI probe at 350°C. The sheath gas flow was 40 units, the auxiliary gas flow was 15 units, and the sweep gas flow was 1 unit. MS data was collected in a range of m/z = 500 –1000. The resolution set at 140,000, the AGC target at $3x10^6$, and the maximum injection time at 250 msec.

H. Data analysis: Metabolites were quantified by integrating peaks using the software TraceFinder 4.1 (ThermoFisher). Metabolites were identified using a 5 ppm mass tolerance, and the expected retention time as determined by an in-house library of chemical standards. ^{13}C and ^{15}N-isotopologues of metabolites were expected to have the same retention time as the ^{12}C and ^{14}N metabolites and were held to the same stringency for mass tolerance (5 ppm). All stable isotope tracing data underwent natural abundance correction using IsoCorrectoR (Bioconductor) (65).

Figure Illustrations: Figures 1A, 1F, 2A, 2D, 3A, 3H, 4A, 4F, S1A, and S11 were all created using Biorender.com.

Reproducibility: All experiments have been carried out at least two independent times. The indicated "n" in figure legends represents biological replicates.

Statistics

Statistical tests are defined in the figure legends. Unless otherwise indicated, a two-tailed student's t-test or a two-way ANOVA was used to compare the means among experimental groups. All statistical tests had an alpha of 0.05 as the significance threshold. * = $P<0.05$.

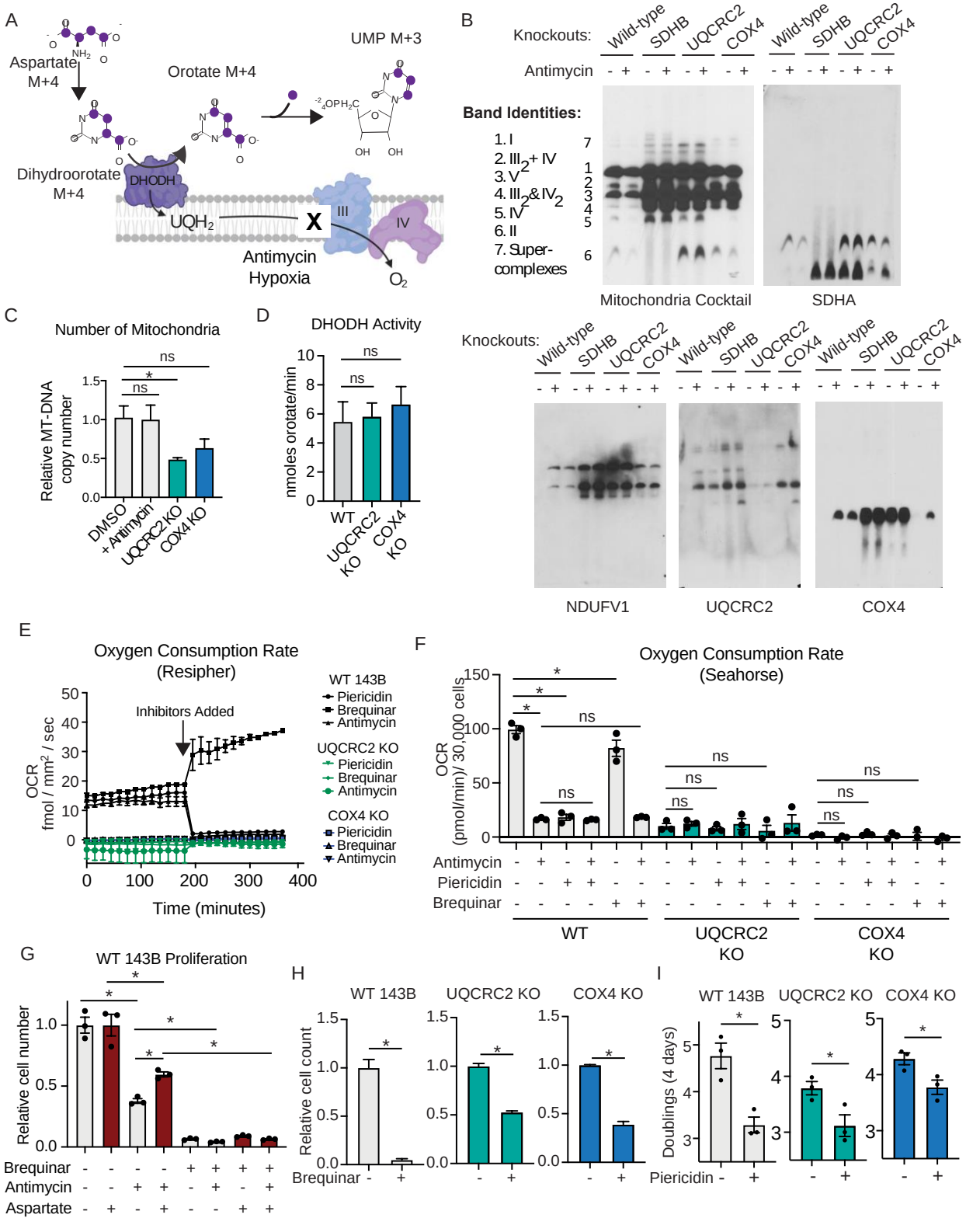

Fig. S1. Cells deficient in O_2 reduction maintain electron input into the ETC.

A. Schematic depicting the incorporation of $^{13}C_4$-aspartate into $^{13}C_3$-UTP. **B.** Immunoblots from blue native gels of mitochondria purified from WT, SDHB KO, UQCRC2 KO, and COX4 KO 143B cells. Immunoblot analyses of indicated proteins using an antibody cocktail that detects components of CI, CII, CIII, CIV, and CV, and individual components of CI (NDUFV1), CII (SDHA), CIII (UQCRC2), and CIV (COX4). Band identities were defined and numbered 1-7. **C**. MT-DNA copy number in WT, UQCRC2 KO, and COX4 KO 143B cells treated with 500 nM antimycin for 2 hours (mean +/- SEM, N=3 per condition) * indicates $P < 0.05$. P values were calculated using a two way ANOVA. **D.** DHODH activity assay performed on lysates from WT, UQCRC2 KO, and COX4 KO 143B cells. Rate of orotate produced overtime is reported (mean +/- SEM, N=6 per condition) * indicates $P < 0.05$. P values were calculated using a two way ANOVA. **E.** O_2 consumption rate (OCR) measured on the Resipher of WT, UQCRC2 KO, and COX4 KO 143B cells. Inhibitors were added at the defined timepoint and OCR was continuously monitored for an additional 3.5 hours. **F.** O_2 consumption rate (OCR) measured on the Seahorse of WT, UQCRC2 KO, and COX4 KO 143B cells treated with either DMSO, 500 nM antimycin, 500 nM piericidin, or 2 μM brequinar for 1 hour (mean +/- SEM, N=3 per condition). * indicates $P < 0.05$. P values were calculated using a two way ANOVA. **G.** Proliferation of WT 143B cells treated with either DMSO, 500 nM antimycin, or 2 μM brequinar for 6 days in the presence or absence of medium supplemented with 10 mM aspartate (mean +/- SEM, N=3 per condition). * indicates $P < 0.05$. P values were calculated using a two way ANOVA. **H.** Proliferation of WT, UQCRC2 KO, or COX4 KO 143B cells treated with either DMSO or 2 μM brequinar for 6 days in medium supplemented with 10 mM Aspartate (mean +/- SEM, N=3 per condition). * indicates $P < 0.05$. P values were calculated using a parametric t test **I.** Doubling times of WT, UQCRC2 KO, and COX4 KO 143B cells treated with DMSO or 500 nM piericidin for 5 days. (mean +/- SEM, N=3 per condition). * indicates $P < 0.05$. P values were calculated using a parametric t test

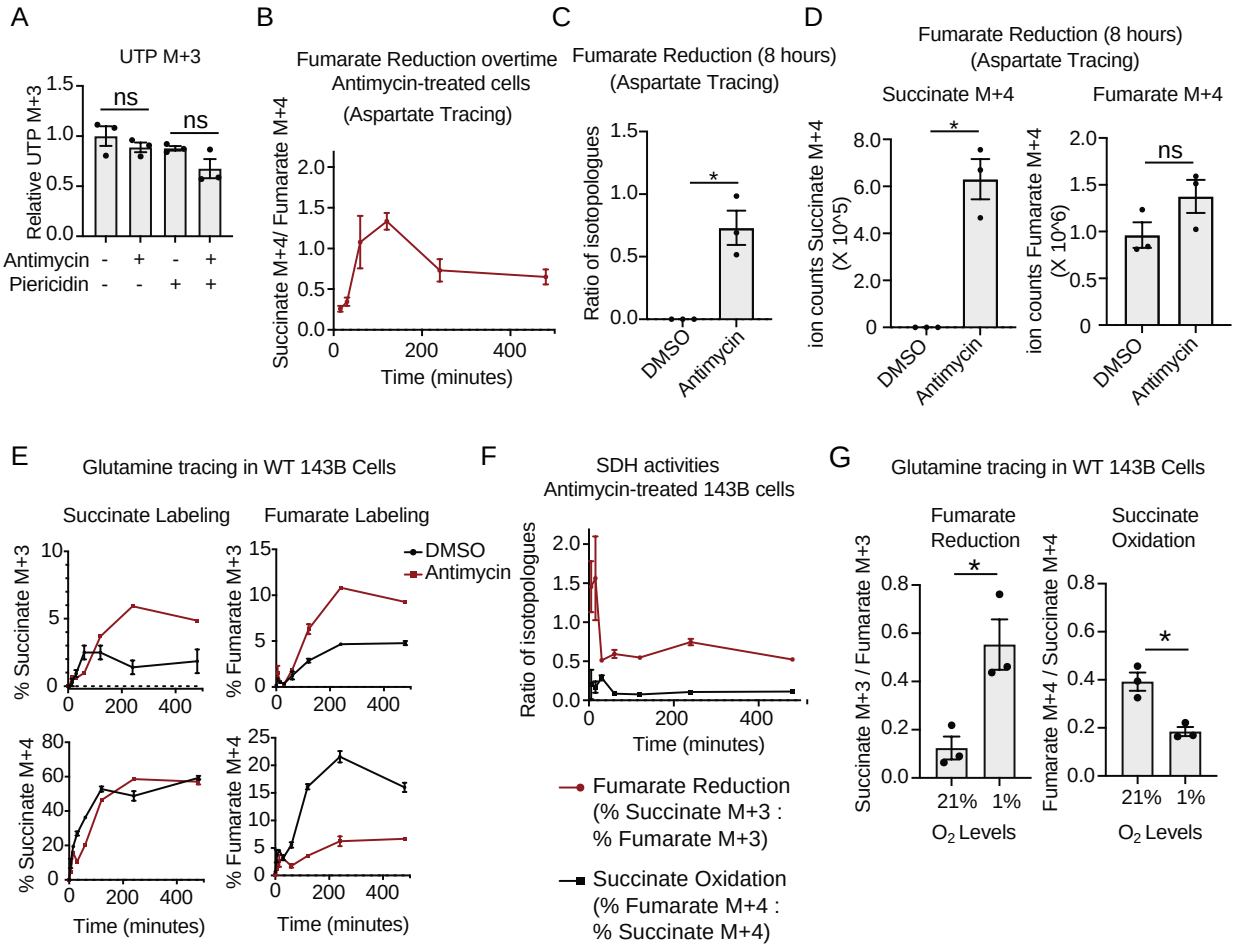

Fig. S2. Fumarate reduction increases and succinate oxidation decreases upon antimycin treatment or hypoxia exposure.

A. The relative ion counts of UTP M+3 from a stable isotope tracing experiment using 10 mM $^{13}C_4$-aspartate in WT 143B cells treated with either DMSO or 500 nM antimycin or 500 nM piericidin for 8 hours (mean +/- SEM, N=3 per condition). **B.** The ratio of % Succinate M+4 to % Fumarate M+4, representing the fumarate reduction reaction from a stable isotope tracing experiment using 3 mM $^{13}C_4$-aspartate. WT 143B cells treated with 500 nM antimycin throughout the depicted time course (mean +/- SEM, N=3 per timepoint). **C.** The ratio of % Succinate M+4 to % Fumarate M+4, representing the fumarate reduction reaction from a stable isotope tracing experiment using 3 mM $^{13}C_4$-aspartate in WT 143B cells treated with either DMSO or 500 nM antimycin for 8 hours (mean +/- SEM, N=3 per condition). **D.** The ion counts of Succinate M+4 and Fumarate M+4 from a stable isotope tracing experiment using 3 mM $^{13}C_4$-aspartate in WT 143B cells treated with either DMSO or 500 nM antimycin for 8 hours (mean +/- SEM, N=3 per condition). **E.** Percent labeled fumarate M+3, fumarate M+4, succinate M+3, and succinate M+4 from a stable isotope tracing experiment using 2 mM $^{13}C_5{}^{15}N_2$-glutamine. WT 143B cells were treated with either DMSO or antimycin for the indicated times (mean +/- SEM, N=3 per timepoint). **F.** The ratio of isotopologues representing the fumarate reduction and succinate oxidation reactions from a stable isotope tracing experiment using 2 mM $^{13}C_5{}^{15}N_2$-glutamine. The ratio for fumarate reduction was calculated by the % succinate M+3 : % fumarate

M+3. The ratio for succinate oxidation was calculated by the % fumarate M+4 : % succinate M+4. WT 143B cells were treated with 500 nM antimycin throughout the depicted time course (mean +/- SEM, N=3 per timepoint). **G.** The ratio of isotopologues representing the fumarate reduction and succinate oxidation reactions from a stable isotope tracing experiment using 2 mM $^{13}C_5{}^{15}N_2$-glutamine. The ratio for fumarate reduction was calculated by the % succinate M+3 : % fumarate M+3. The ratio for succinate oxidation was calculated by the % fumarate M+4 : % succinate M+4. Tracing was performed for 8 hours in WT 143B cells that were pre-adapted to either 21% or 1% O_2 for 48 hours (mean +/- SEM, N=3 per condition).). For all experiments * indicates $P < 0.05$. P values were calculated using an unpaired parametric t test.

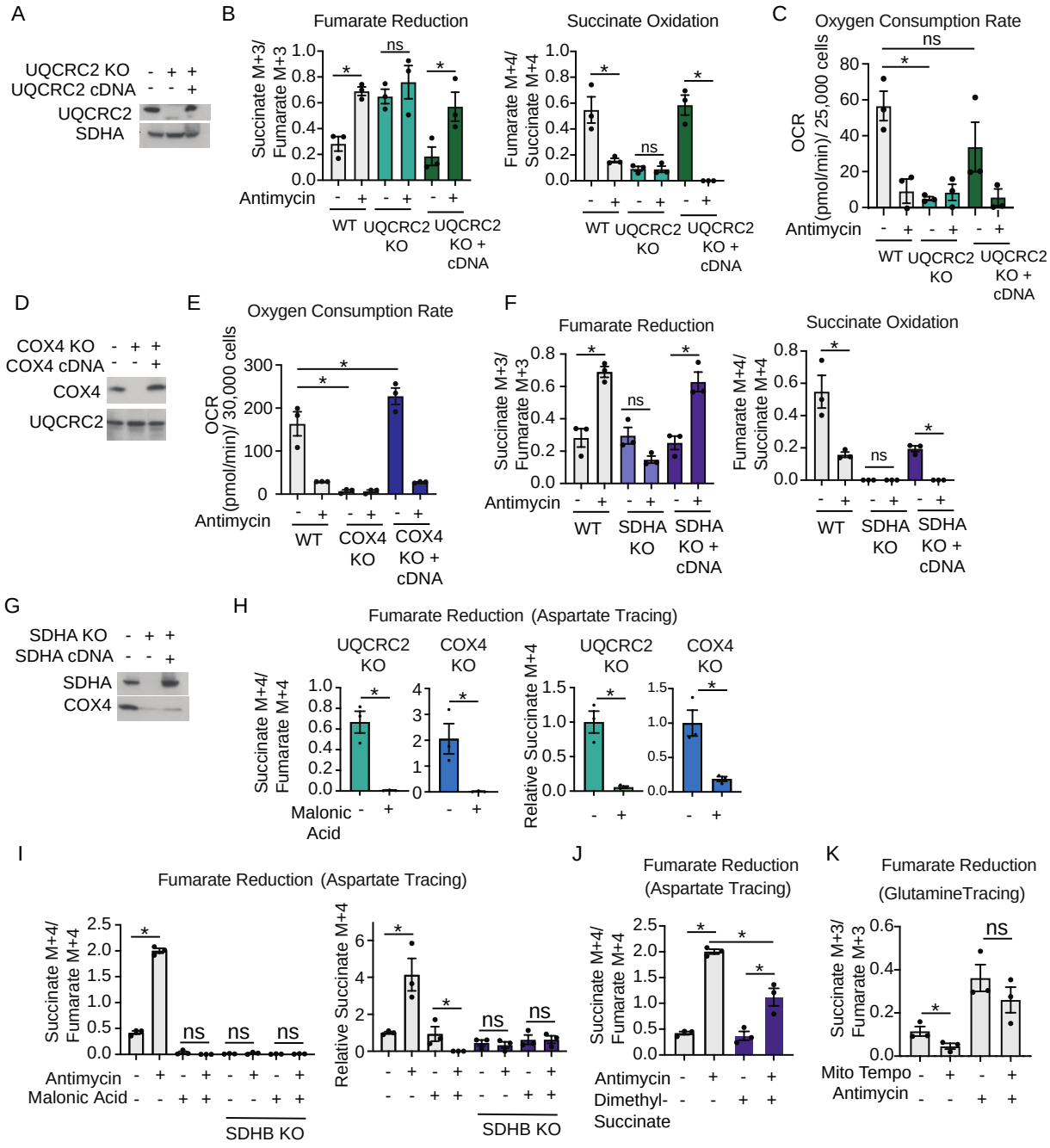

Fig. S3. Upon inhibition of O_2 reduction, fumarate accepts electrons from net-reversal of the SDH complex.

A. Immunoblot analyses for indicated proteins in WT, UQCRC2 KO, and UQCRC2 KO 143B cells expressing the UQCRC2 cDNA. **B.** The ratio of isotopologues representing the fumarate

reduction and succinate oxidation reactions from a stable isotope tracing experiment using 2 mM $^{13}C_5{}^{15}N_2$-glutamine. The ratio for fumarate reduction was calculated by the % succinate M+3 : % fumarate M+3. The ratio for succinate oxidation was calculated by the % fumarate M+4 : % succinate M+4. Tracing was performed for 8 hours in WT, UQCRC2 KO, and UQCRC2 KO with cDNA add back 143B cells treated with either DMSO or 500 nM antimycin (mean +/- SEM, N=3 per condition). **C.** O_2 consumption rate of WT, UQCRC2 KO, and UQCRC2 cDNA-addback 143B cells treated with DMSO or 500 nM antimycin for 1 hour (mean +/- SEM, N=3 per condition). * indicates $P < 0.05$. P values were calculated using a two way ANOVA. **D.** Immunoblot analyses for indicated proteins in WT, COX4 KO, and COX4 KO 143B cells expressing the COX4 cDNA. **E.** O_2 consumption rates of WT, COX4 KO, and COX4 cDNA addback 143B cells treated with DMSO or 500 nM antimycin for 1 hour (mean +/- SEM, N=3 per condition). * indicates $P < 0.05$. P values were calculated using a two way ANOVA. **F.** The ratio of isotopologues representing the fumarate reduction and succinate oxidation reactions from a stable isotope tracing experiment using 2 mM $^{13}C_5{}^{15}N_2$-glutamine. The ratio for fumarate reduction was calculated by the % succinate M+3 : % fumarate M+3. The ratio for succinate oxidation was calculated by the % fumarate M+4 : % succinate M+4. Tracing was performed for 8 hours in WT, SDHA KO, and SDHA KO with cDNA add back 143B cells treated with either DMSO or 100 nM antimycin (mean +/- SEM, N=3 per condition). **G.** Immunoblot analyses for indicated proteins of WT, SDHA KO, and SDHA KO 143B cells expressing the SDHA cDNA. **H.** The ratio of isotopologues representing fumarate reduction and relative ion counts of succinate M+4 from a stable isotope tracing experiment using 5 mM $^{13}C_4$-aspartate. The ratio for fumarate reduction was calculated by the % succinate M+4 : % fumarate M+4. Tracing was performed for 8 hours in WT 143B cells treated with either DMSO, 500 nM antimycin, or 20 mM malonic acid (mean +/- SEM, N=3 per condition). **I.** The ratio of isotopologues representing fumarate reduction and the relative ion counts of succinate M+4 from a stable isotope tracing experiment using 5 mM $^{13}C_4$-aspartate. The ratio for fumarate reduction was calculated by the % succinate M+4 : % fumarate M+4. Tracing was performed for 8 hours in WT and SDHB KO 143B cells treated with either DMSO, 500 nM antimycin, or 20 mM malonic acid (mean +/- SEM, N=3 per condition). **J.** The ratio of isotopologues representing fumarate reduction from a stable isotope tracing experiment using 5 mM $^{13}C_4$-aspartate. The ratio for fumarate reduction was calculated by the % succinate M+4 : % fumarate M+4. Tracing was performed for 8 hours in WT 143B cells treated with either DMSO, 500 nM antimycin, or 10 mM dimethyl succinate (mean +/- SEM, N=3 per condition). * indicates $P < 0.05$. P values were calculated using a two way ANOVA. **K.** The ratio of isotopologues representing fumarate reduction from a stable isotope tracing experiment using 2 mM $^{13}C_5{}^{15}N_2$-glutamine. The ratio for fumarate reduction was calculated by the % succinate M+3 : % fumarate M+3. Tracing was performed for 8 hours in WT 143B cells treated with either DMSO, 500 nM antimycin, or 25 μM MitoTEMPO (mean +/- SEM, N=3 per condition). For all experiments * indicates $P < 0.05$. P values were calculated using an unpaired parametric t test unless otherwise stated.

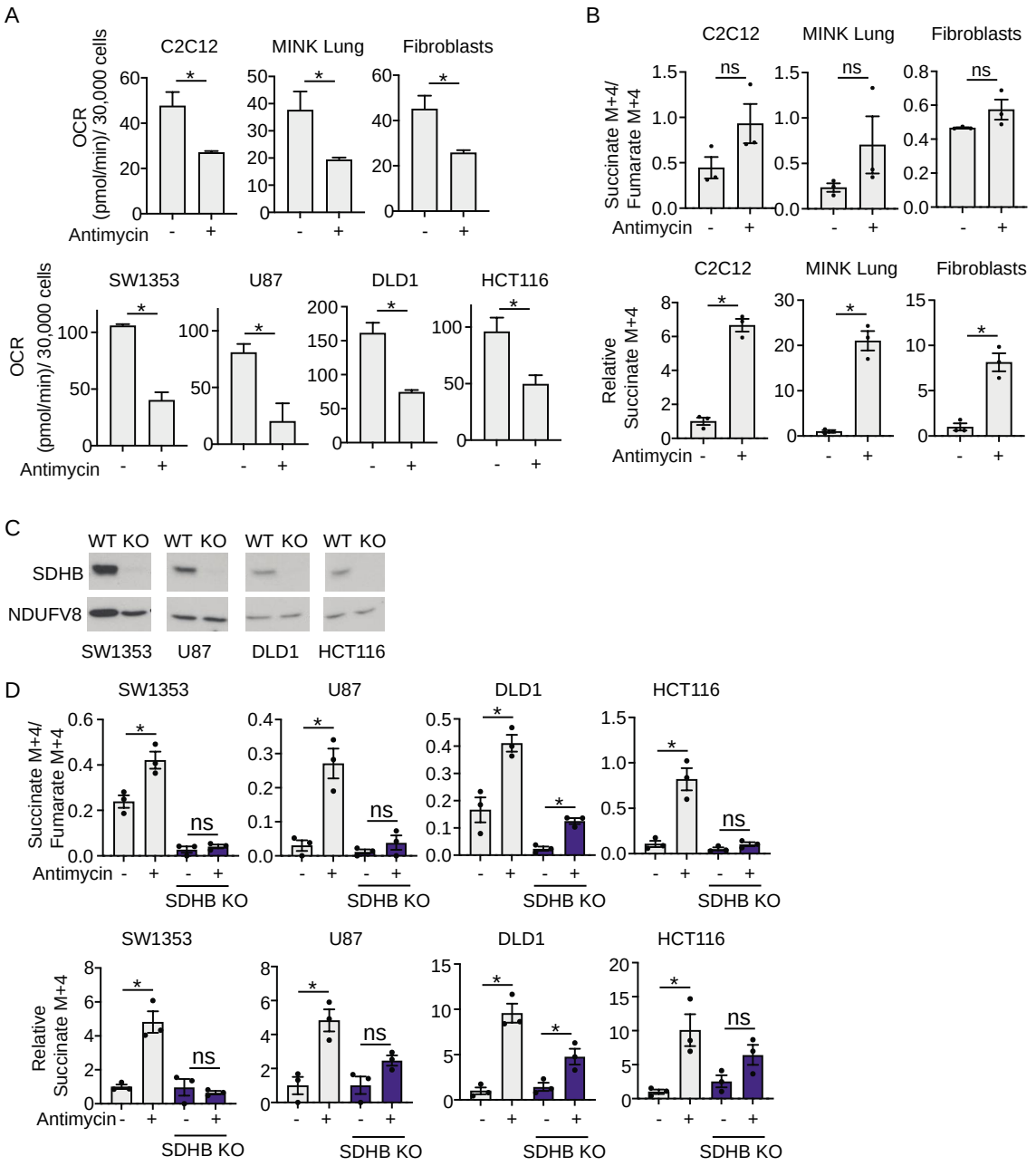

Fig. S4. Upon inhibition of O_2 reduction, fumarate accepts electrons from net-reversal of the SDH complex in a panel of cell lines

A. O_2 consumption rate of the listed cell lines treated with DMSO or 500 nM antimycin for 1 hour (mean +/- SEM, N=3 per condition). **B.** The ratio of isotopologues representing fumarate reduction and the relative ion counts of succinate M+4 from a stable isotope tracing experiment using 10 mM $^{13}C_4$-aspartate. The ratio for fumarate reduction was calculated by the % succinate M+4 : % fumarate M+4. Tracing was performed for 8 hours in cells treated with either DMSO or 500 nM antimycin (mean +/- SEM, N=3 per condition). **C.** Immunoblot analyses for indicated

proteins in WT and SDHB KO cells in a panel of cell lines with population knockout of SDHB. **D.** The ratio of isotopologues representing fumarate reduction and the relative ion counts of succinate M+4 from a stable isotope tracing experiment using 10 mM $^{13}C_4$-aspartate. The ratio for fumarate reduction was calculated by the % succinate M+4 : % fumarate M+4. Tracing was performed in WT and SDHB KO cells treated for 8 hours with either DMSO or 500 nM antimycin (mean +/- SEM, N=3 per condition). For all experiments * indicates $P < 0.05$. P values were calculated using an unpaired parametric t test.

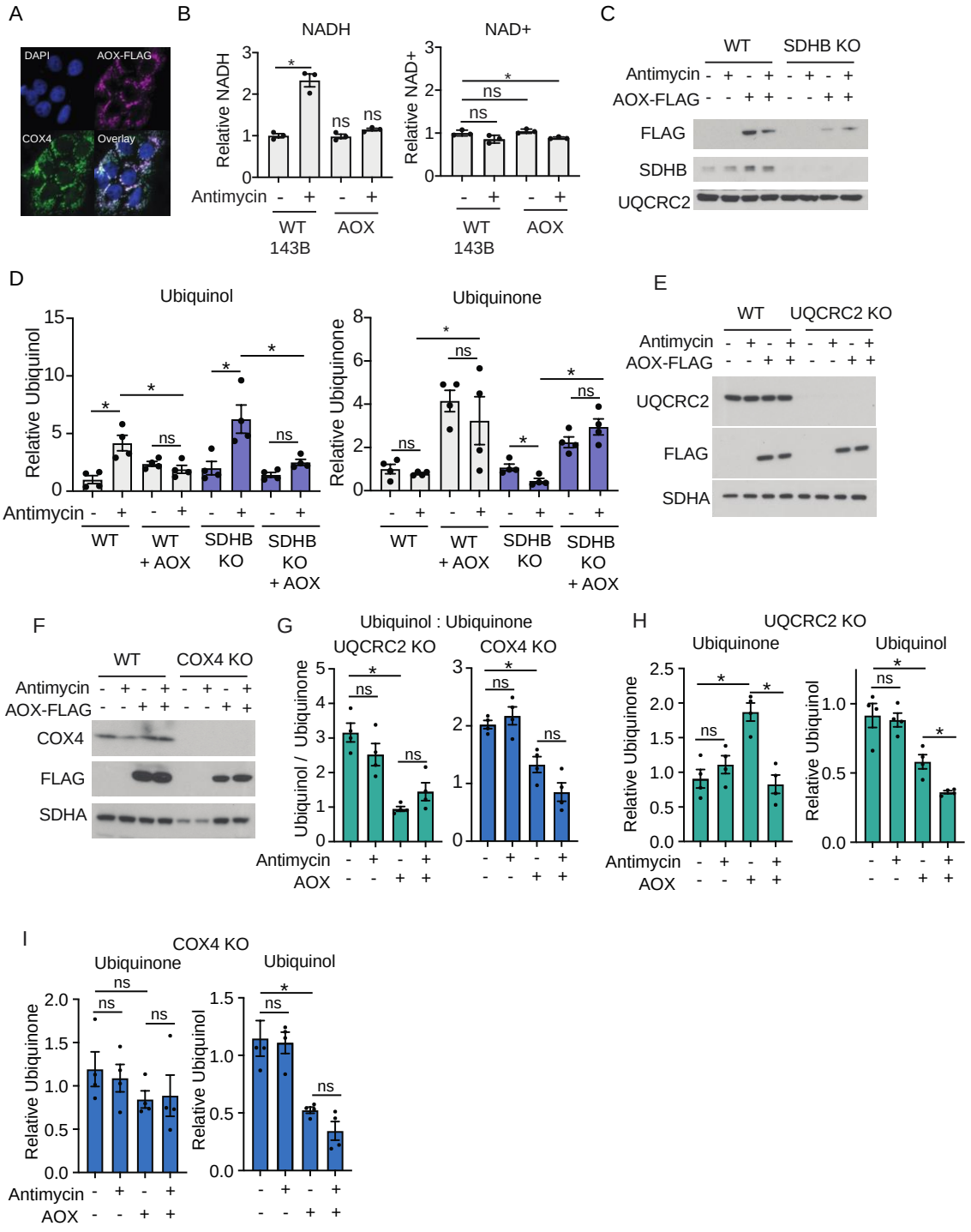

Fig. S5. Expression of alternative oxidase restores the ubiquinol:ubiquinone ratio in 143B cells deficient in fumarate and O_2 reduction in the ETC

A. Immunofluorescence assay showing co-localization of FLAG-tagged AOX with the mitochondrial marker COX4 **B.** NADH and NAD+ measured by mass spectrometry in 143B cells expressing AOX and treated with DMSO or 500 nM antimycin for 8 hours (mean +/- SEM, N=3 per condition). * indicates $P < 0.05$. P values were calculated using a two way ANOVA **C.** Immunoblot analysis of AOX expression in WT and SDHB KO cells treated with DMSO or 500 nM antimycin for 2 hours. **D.** Relative ion counts for ubiquinol and ubiquinone in mitochondria isolated from WT and SDHB KO 143B cells expressing AOX-FLAG and treated with DMSO or antimycin for 4 hours (mean +/- SEM, N=4 per condition). * indicates $P < 0.05$. P values were calculated using a two way ANOVA **E-F.** Immunoblot analyses for indicated proteins in WT and UQCRC2 KO 143B cells (E) or COX4 KO 143B cells (F) with or without AOX expression and treated with DMSO or 500 nM antimycin for 2 hours. **G.** Ratio of ubiquinol ion counts to ubiquinone ion counts from mitochondrial isolated from UQCRC2 KO and COX4 KO cells with or without expression of AOX and treated with DMSO or 500 nM antimycin for 4 hours (mean +/- SEM, N=4 per condition). * indicates $P < 0.05$. P values were calculated using a two way ANOVA **H-I.** Relative ion counts for ubiquinol and ubiquinone in mitochondria isolated from UQCRC2 KO (H) or COX4 KO (I) 143B cells expressing AOX-FLAG and treated with DMSO or antimycin for 4 hours (mean +/- SEM, N=4 per condition). * indicates $P < 0.05$. P values were calculated using a two way ANOVA

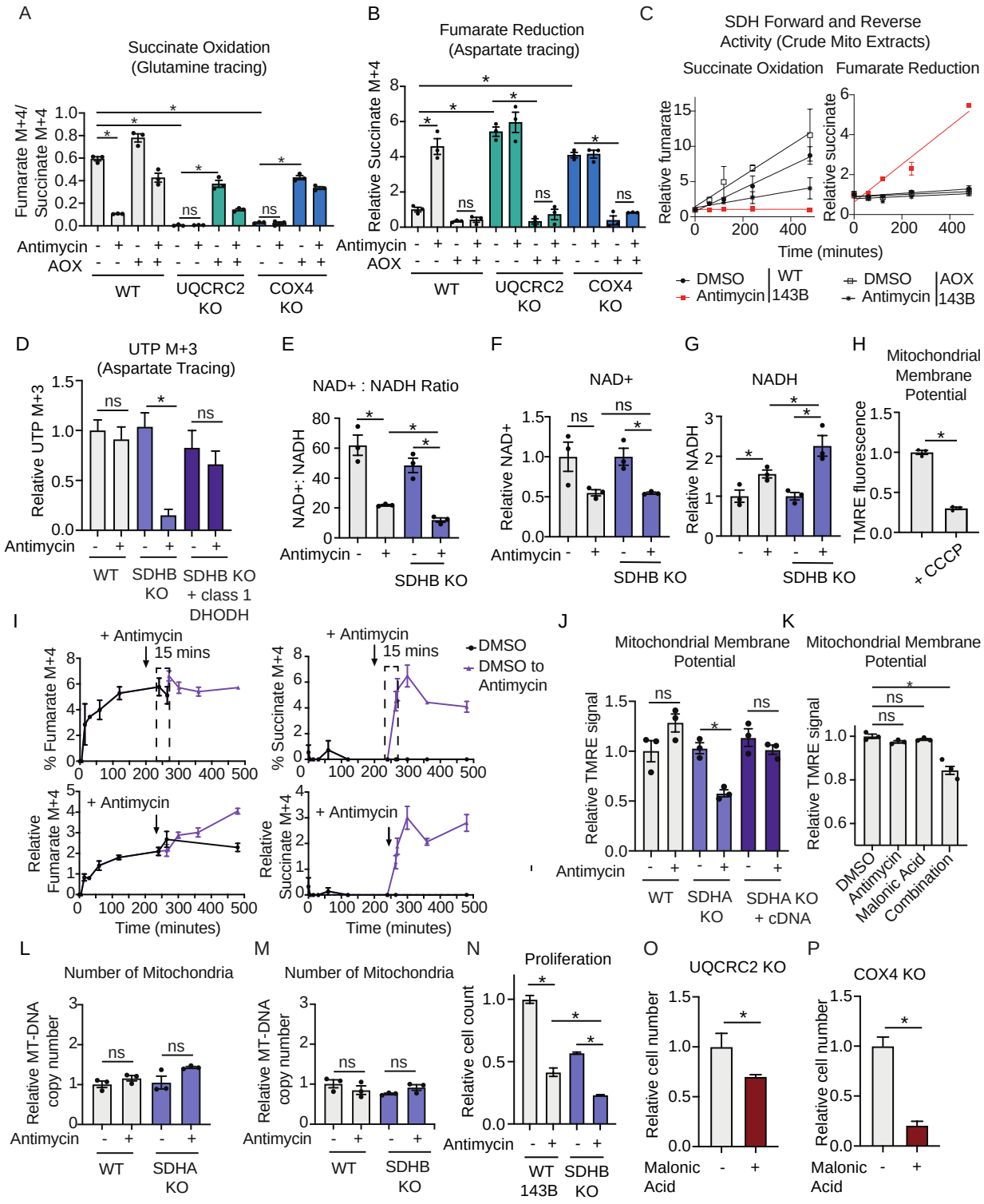

Fig. S6. Fumarate reduction is required to maintain nucleotide biosynthesis and the mitochondrial membrane potential in cells deficient in O_2 reduction

A. The ratio of isotopologues representing succinate oxidation from a stable isotope tracing experiment using 2 mM $^{13}C_5{}^{15}N_2$-glutamine. The ratio for succinate oxidation was calculated by

the % fumarate M+4 : % succinate M+4. Tracing was performed for 8 hours in WT, UQCRC2 KO, and COX4 KO 143B cells expressing or not expressing AOX and treated with DMSO or 500 nM antimycin (mean +/- SEM, N=3 per condition). * indicates $P < 0.05$. P values were calculated using a two way ANOVA **B.** The relative ion counts of succinate M+4 from a stable isotope tracing experiment using 10 mM $^{13}C_4$-aspartate. Tracing was performed for 8 hours in cells treated with either DMSO or 500 nM antimycin (mean +/- SEM, N=3 per condition). * indicates $P < 0.05$. P values were calculated using a two way ANOVA **C.** SDH activity in purified mitochondria from WT and AOX-expressing 143B cells. DMSO or 1 μM antimycin were added where indicated (mean +/- SEM, N=3 per condition). Data points were fitted using linear regression. **D.** DHODH activity as measured by stable isotope tracing with 10 mM $^{13}C_4$-aspartate, which generates $^{13}C_3$-UTP if DHODH is active. Tracing was for 8 hours in WT, SDHB KO, and KO 143B cells expressing a codon optimized class 1 DHODH cDNA from Trypanosoma cruzi and treated with DMSO or 500 nM antimycin (mean +/- SEM, N=3 per condition). **E-G.** The ratio of NAD+ and NADH ion counts (E) and relative ion counts of NAD+ (F) and NADH (G) in WT and SDHB KO 143B cells treated with either DMSO or 500 nM antimycin for 8 hours (mean +/- SEM, N=3 per condition). * indicates $P < 0.05$. P values were calculated using a two way ANOVA **H.** Mitochondrial membrane potential in 143B cells treated with DMSO or 250 nM CCCP for 1 hour (mean +/- SEM, N=3 per condition). **I.** Percent and relative labeled fumarate M+4 and succinate M+4 from a stable isotope tracing experiment using 3 mM $^{13}C_4$-aspartate. WT 143B cells were treated with DMSO or antimycin at the indicated times (mean +/- SEM, N=3 per timepoint). **J.** Mitochondrial membrane potential in WT, SDHA KO, and SDHA KO cells expressing the SDHA cDNA and treated with DMSO or 500 nM antimycin for 2 hours (mean +/- SEM, N=3 per condition). **K.** Mitochondrial membrane potential in 143B cells treated with DMSO, 500 nM antimycin, 10 mM Malonic acid, or the combination for 1 hour (mean +/- SEM, N=3 per condition). * indicates $P < 0.05$. P values were calculated using a two way ANOVA **L-M.** MT-DNA copy number in WT, or SDHA (L) or SDHB (M) KO 143B cells treated with 500 nM antimycin for 2 hours (mean +/- SEM, N=3 per condition). **N**. Proliferation of WT and SDHB KO 143B cells treated with either DMSO or 500 nM antimycin for 6 days in medium supplemented with 10 mM Aspartate (mean +/- SEM, N=3 per condition). * indicates $P < 0.05$. P values were calculated using a two way ANOVA **O-P**. Proliferation of UQCRC2 KO (O) and COX4 KO (P) 143B cells untreated or treated with 20 mM malonic acid for 6 days in medium supplemented with 10 mM aspartate and 5 mM pyruvate (mean +/- SEM, N=3 per condition). For all experiments * indicates $P < 0.05$. P values were calculated using an unpaired parametric t test unless otherwise stated.

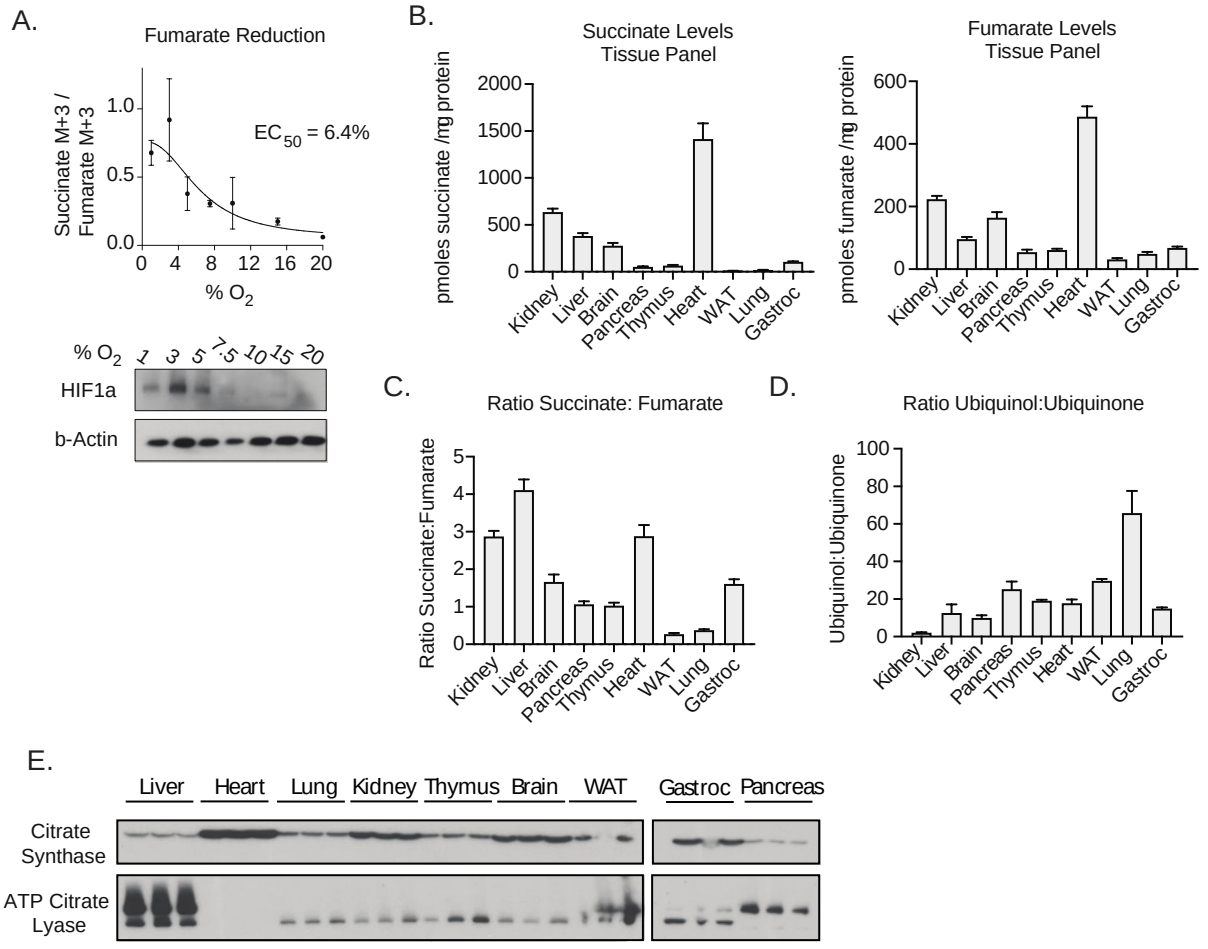

Fig. S7. **Fumarate reduction is heterogeneous *in vivo***

A. The ratio of isotopologues representing the fumarate reduction from a stable isotope tracing experiment using 2 mM $^{13}C_5{}^{15}N_2$-glutamine. The ratio for fumarate reduction was calculated by the % succinate M+3 : % fumarate M+3. Fumarate reduction was measured by tracing $^{13}C_5{}^{15}N_2$-glutamaine for 8 hours in 143B cells at the indicated O_2 concentrations. Cells were conditioned to O_2 levels for 24 hours prior to experimentation (mean +/- SEM, N=3 per condition). Immunoblot analyses of HIF1α expression in cells at each O_2 concentration. **B**. Absolute quantification of the succinate and fumarate levels in tissues from male and female mice 10-12 weeks old (mean +/- SEM, N=16 per condition). Data are reported as pmoles of the metabolite per μg of tissue protein. **C.** The ratio of the absolute quantification of succinate and fumarate levels in tissues from male and female mice 10-12 weeks old (mean +/- SEM, N=16 per condition). The ratio was calculated by dividing the pmoles succinate per μg of tissue protein by the pmoles fumarate per μg of tissue protein. **D.** Ratio of ubiquinol ion counts to ubiquinone ion counts from mitochondrial isolated from tissues from wild-type female mice 12 weeks old (mean +/- SEM, N=4 per condition). **E.** Immunoblot analyses of citrate synthase and ATP citrate lyase in 30 μg of tissue protein from three wild-type female mice 12 weeks old.

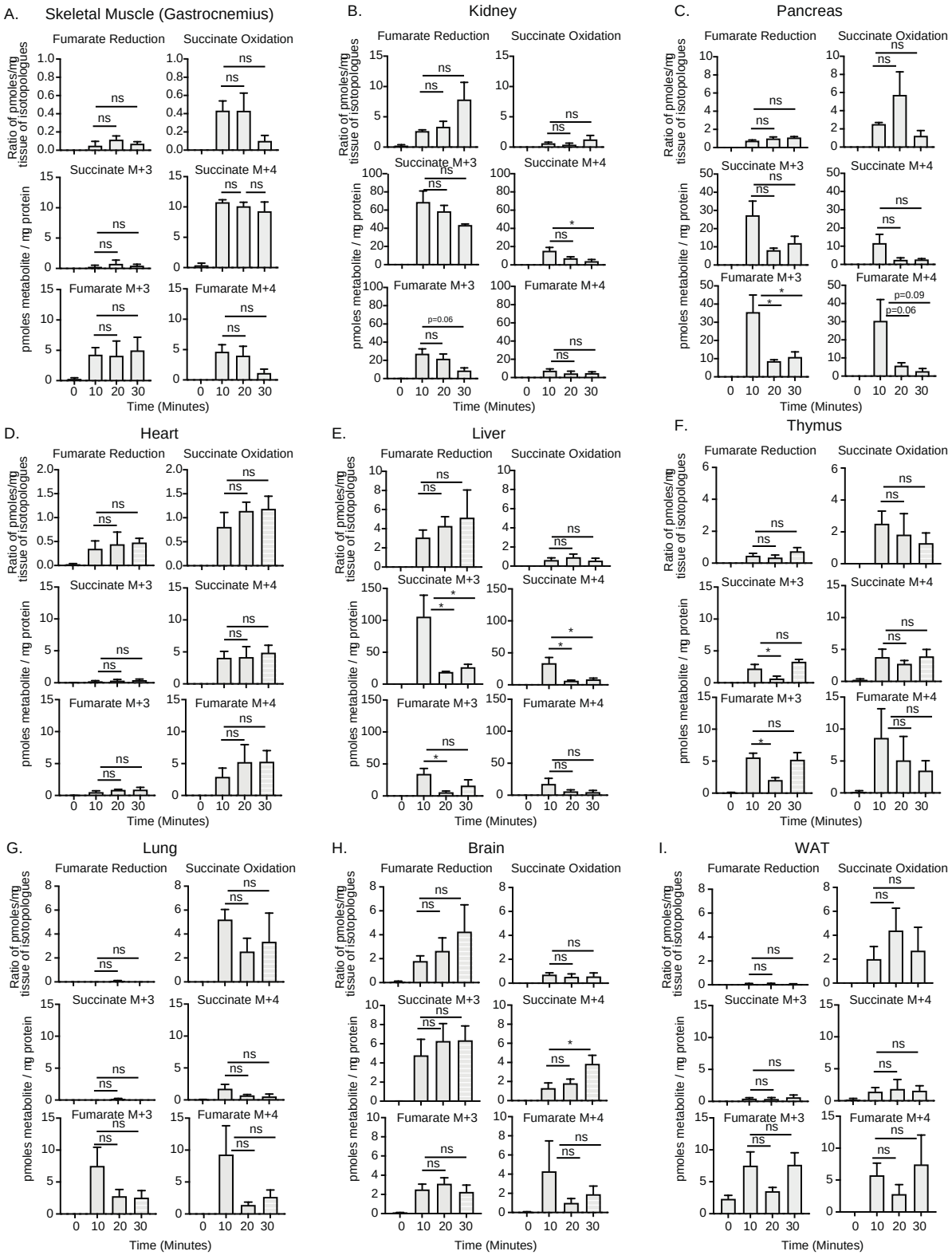

Fig. S8. Fumarate reduction and succinate oxidation reactions measured *in vivo* by $^{13}C_5{}^{15}N_2$-glutamine tracing

In vivo $^{13}C_5{}^{15}N_2$-glutamine tracing in female mice 10 weeks old via retroorbital and intraperitoneal injections. Mice were euthanized 10, 20, and 30 minutes after injections and tissues were harvested for metabolite isolation and mass spectrometry. Absolute quantification was performed to calculate the concentration of succinate M+3, succinate M+4, fumarate M+3, and fumarate M+4 in pmoles per μg tissue protein. The reported ratio representing fumarate reduction was calculated by the pmoles succinate M+3 per μg tissue protein : the pmoles fumarate M+3 per μg tissue protein. The reported ratio representing succinate oxidation was calculated by the pmoles fumarate M+4 per μg tissue protein : the pmoles succinate M+4 per μg tissue protein. Data represent the mean +/- SEM, N=4 mice per timepoint. For all experiments * indicates $P < 0.05$. P values were calculated using a two way ANOVA.

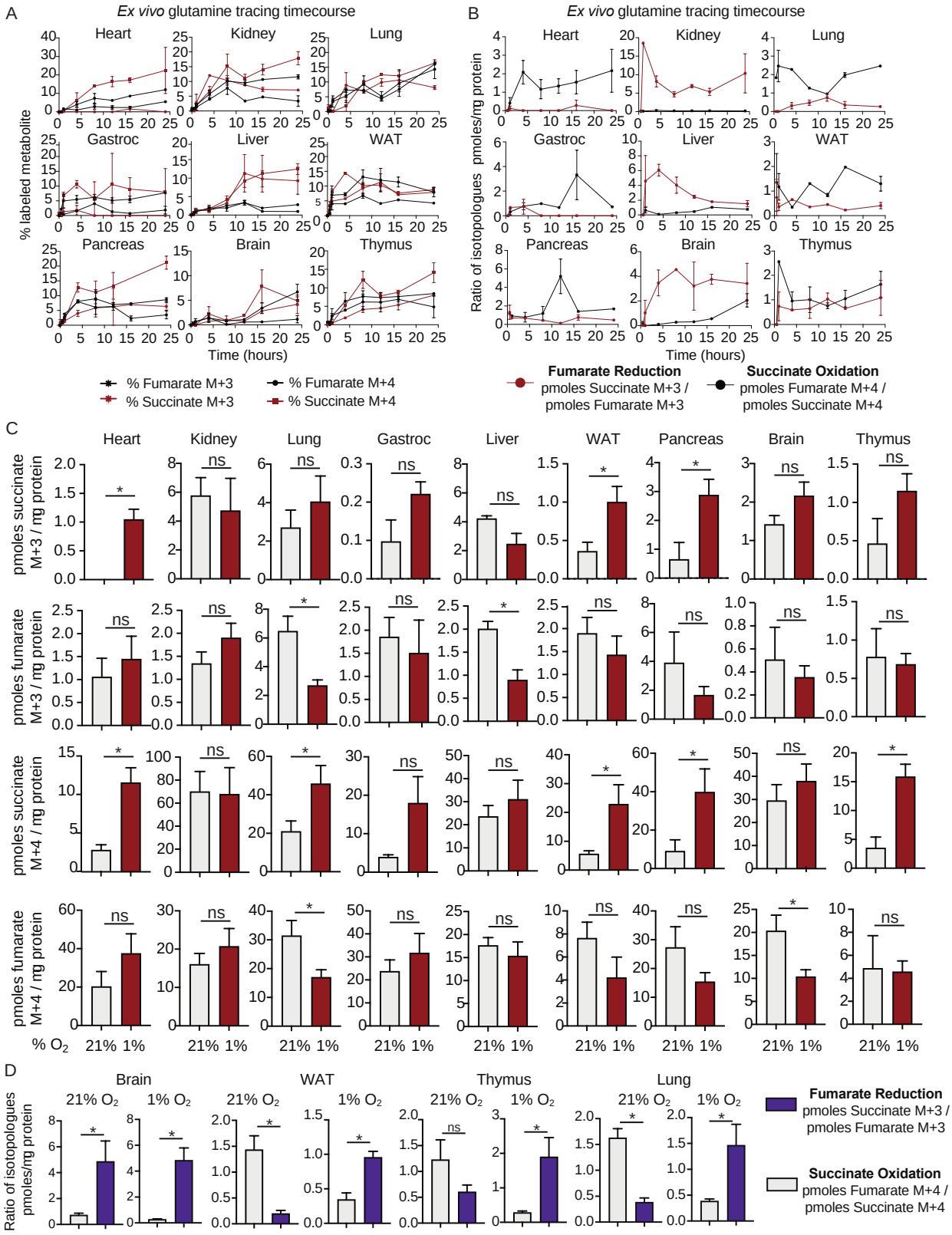
A
Ex vivo glutamine tracing timecourse
Heart
Kidney
Lung
Gastroc
Liver
WAT
Pancreas
Brain
Thymus
% labeled metabolite
Time (hours)
% Fumarate M+3
% Succinate M+3
% Fumarate M+4
% Succinate M+4
B
Ex vivo glutamine tracing timecourse
Ratio of isotopologues pmoles/mg protein
Time (hours)
Fumarate Reduction
pmoles Succinate M+3 / pmoles Fumarate M+3
Succinate Oxidation
pmoles Fumarate M+4 / pmoles Succinate M+4
C
pmoles succinate M+3 / mg protein
pmoles fumarate M+3 / mg protein
pmoles succinate M+4 / mg protein
pmoles fumarate M+4 / mg protein
% O2
21% 1%
ns
D
Brain
WAT
Thymus
Lung
21% O2
1% O2
Ratio of isotopologues pmoles/mg protein
Fumarate Reduction
pmoles Succinate M+3 / pmoles Fumarate M+3
Succinate Oxidation
pmoles Fumarate M+4 / pmoles Succinate M+4

Fig. S9. *Ex vivo* glutamine tracing reveals that the SDH complex undergoes a net-reversal upon hypoxia exposure in many mouse tissues

A. Percent labeled fumarate M+3, fumarate M+4, succinate M+3, and succinate M+4 from a stable isotope tracing experiment using 5 mM $^{13}C_5{}^{15}N_2$-glutamine on tissues dissected from female mice and cultured *ex vivo* (mean +/- SEM, N=3 per timepoint). **B.** $^{13}C_5{}^{15}N_2$-glutamine tracing time course on tissues dissected from female mice and cultured *ex vivo.* Absolute quantification was performed to calculate the concentration of succinate M+3, succinate M+4, fumarate M+3, and fumarate M+4 in pmoles per μg tissue protein. The reported ratio representing fumarate reduction was calculated by the pmoles succinate M+3 per μg tissue protein : the pmoles fumarate M+3 per μg tissue protein. The reported ratio representing succinate oxidation was calculated by the pmoles fumarate M+4 per μg tissue protein : the pmoles succinate M+4 per μg tissue protein (mean +/- SEM, N=3 per timepoint). **C.** *Ex vivo* $^{13}C_5{}^{15}N_2$-glutamine tracing in the indicated tissues for 24 hours in a normoxia incubator (21% O_2) or hypoxia incubator (1% O_2) (mean +/- SEM, N=4 per condition). Absolute quantification was performed to calculate the concentration of succinate M+3, succinate M+4, fumarate M+3, and fumarate M+4 in pmoles per μg tissue protein. **D.** *Ex vivo* $^{13}C_5{}^{15}N_2$-glutamine tracing in the indicated tissues for 24 hours in a normoxia incubator (21% O_2) or hypoxia incubator (1% O_2) (mean +/- SEM, N=4 per condition). Absolute quantification was performed to calculate the concentration of succinate M+3, succinate M+4, fumarate M+3, and fumarate M+4 in pmoles per μg tissue protein. The reported ratio representing fumarate reduction was calculated by the pmoles succinate M+3 per μg tissue protein : the pmoles fumarate M+3 per μg tissue protein. The reported ratio representing succinate oxidation was calculated by the pmoles fumarate M+4 per μg tissue protein : the pmoles succinate M+4 per μg tissue protein. Data represent the mean +/- SEM, N=4 mice per timepoint. For all experiments * indicates $P < 0.05$. P values were calculated using an unpaired parametric t test.

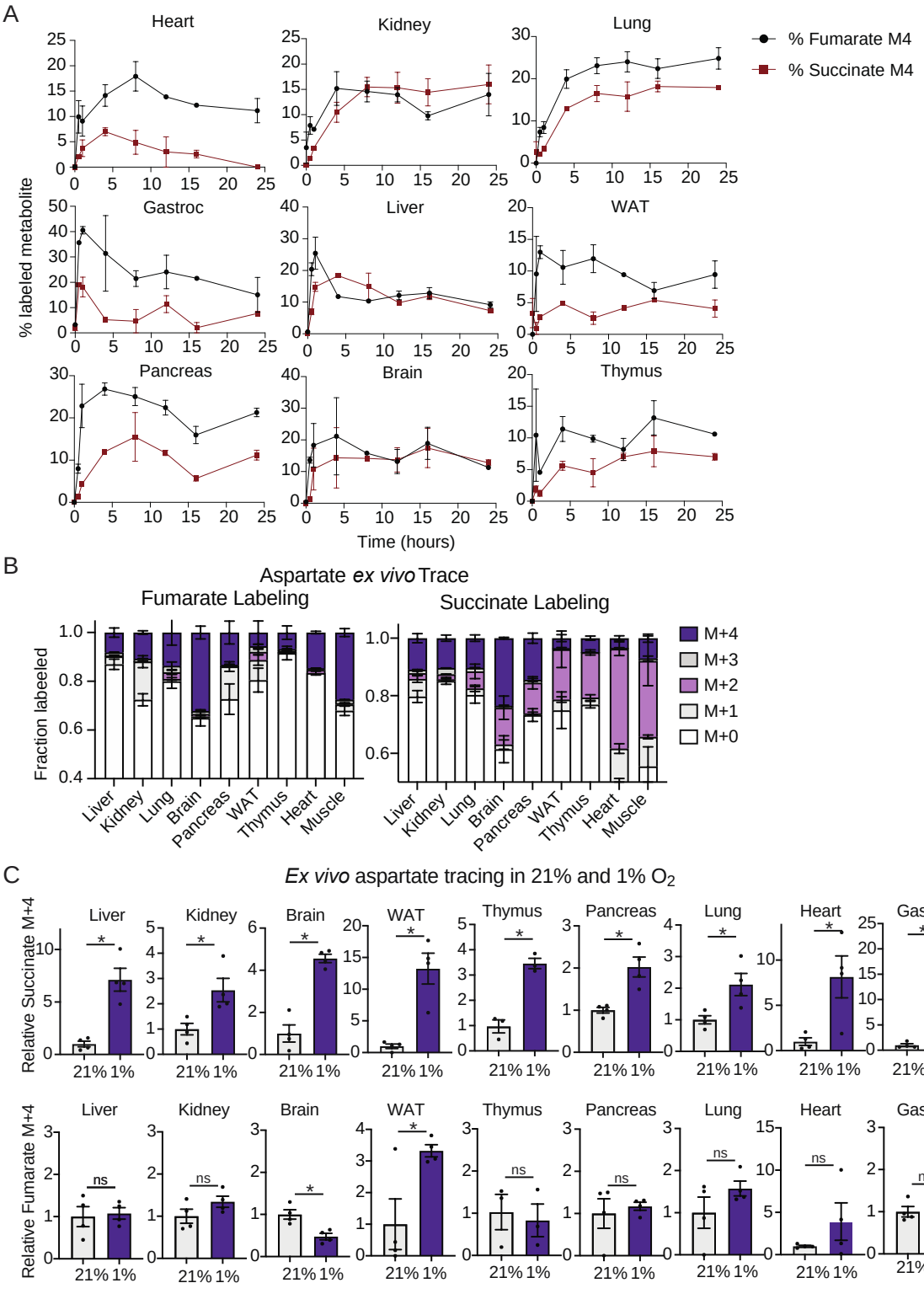
A
Heart
Kidney
Lung
Gastroc
Liver
WAT
Pancreas
Brain
Thymus
% Fumarate M4
% Succinate M4
% labeled metabolite
Time (hours)
B
Aspartate ex vivo Trace
Fumarate Labeling
Succinate Labeling
Fraction labeeled
M+4
M+3
M+2
M+1
M+0
Liver
Kidney
Lung
Brain
Pancreas
WAT
Thymus
Heart
Muscle
C
Ex vivo aspartate tracing in 21% and 1% O2
Relative Succinate M+4
Relative Fumarate M+4
21%
1%
ns

Fig. S10. *Ex vivo* aspartate tracing reveals that fumarate reduction increases in mouse tissues exposed to hypoxia

A. Percent labeled fumarate M+4 and succinate M+4 from a stable isotope tracing experiment using 10 mM $^{13}C_4$-aspartate on tissues dissected from 14 week old male mice and cultured *ex vivo* (mean +/- SEM, N=2 per timepoint). **B.** Percent labeled fumarate M+4 and succinate M+4 from a stable isotope tracing experiment using 10 mM $^{13}C_4$-aspartate for 16 hours in the indicated tissues kept *ex vivo* in a tissue culture incubator (21% O_2). Succinate M+4 generation reflects fumarate reduction (mean +/- SEM, N=4 per condition). **C.** *Ex vivo* $^{13}C_4$-aspartate tracing in the indicated tissues for 16 hours in a normoxia incubator (21% O_2) or hypoxia incubator (1% O_2) (mean +/- SEM, N=4 per condition). Relative ion counts for succinate M+4 and fumarate M+4 are reported. For all experiments * indicates $P < 0.05$. P values were calculated using an unpaired parametric t test.

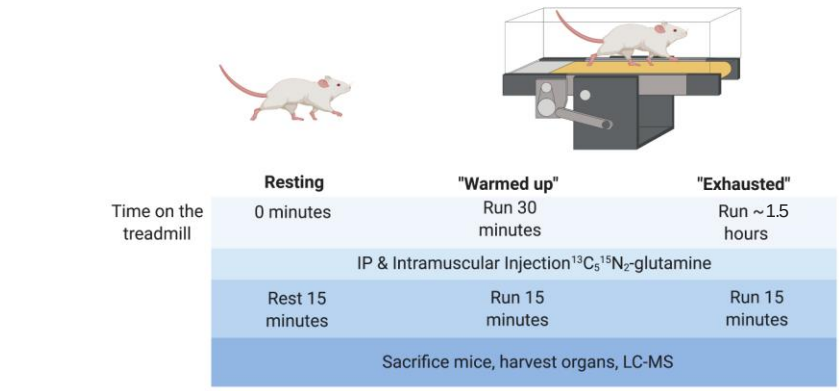
Resting
"Warmed up"
"Exhausted"
Time on the treadmill
0 minutes
Run 30 minutes
Run ~1.5 hours
IP & Intramuscular Injection $^{13}C_5{}^{15}N_2$-glutamine
Rest 15 minutes
Run 15 minutes
Run 15 minutes
Sacrifice mice, harvest organs, LC-MS

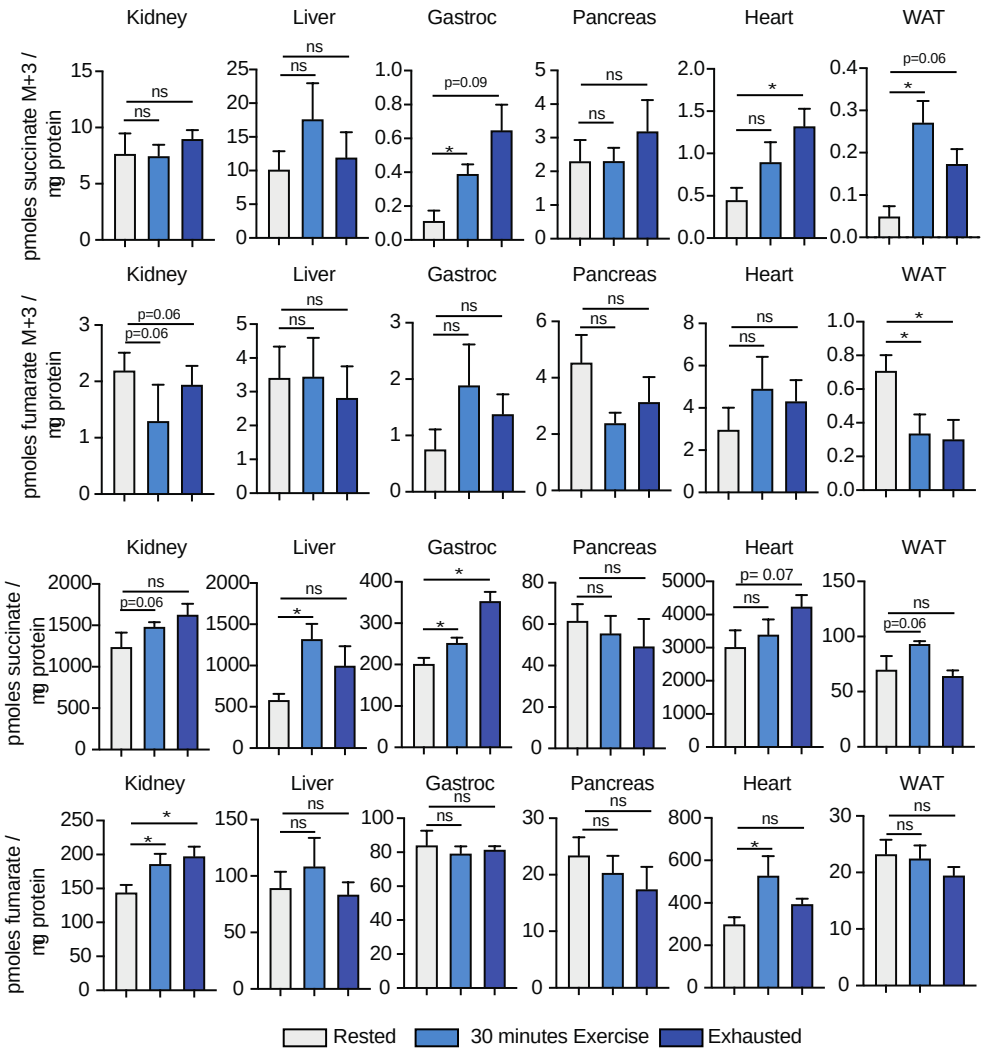
Kidney
Liver
Gastroc
Pancreas
Heart
WAT
pmoles succinate M+3 / mg protein
pmoles fumarate M+3 / mg protein
pmoles succinate / mg protein
pmoles fumarate / mg protein
ns
p=0.09
p=0.06
p= 0.07
Rested
30 minutes Exercise
Exhausted

Fig. S11. Fumarate reduction is increased upon exercise challenge in many mouse tissues

In vivo $^{13}C_5{}^{15}N_2$-glutamine tracing in female mice 12 weeks old via intraperitoneal and intramuscular injections. Mice were either rested, exercised for 30 minutes, or until exhaustion for approximately 1.5 hours and then injected with $^{13}C_5{}^{15}N_2$-glutamine. Post injection the rested mice were euthanized 15 minutes later with no exercise, and the exercised mice continued to run on the treadmill for 15 minutes before being euthanized. Tissues were harvested for metabolite isolation and mass spectrometry. Absolute quantification was performed to calculate the concentration of succinate M+3, succinate M+4, fumarate M+3, and fumarate M+4 in pmoles per μg tissue protein. The reported ratio representing fumarate reduction was calculated by the pmoles succinate M+3 per μg tissue protein : the pmoles fumarate M+3 per μg tissue protein. The reported ratio representing succinate oxidation was calculated by the pmoles fumarate M+4 per μg tissue protein : the pmoles succinate M+4 per μg tissue protein. Data represent the mean +/- SEM, N=5 mice per timepoint. * indicates $P < 0.05$. P values were calculated using a two way ANOVA.

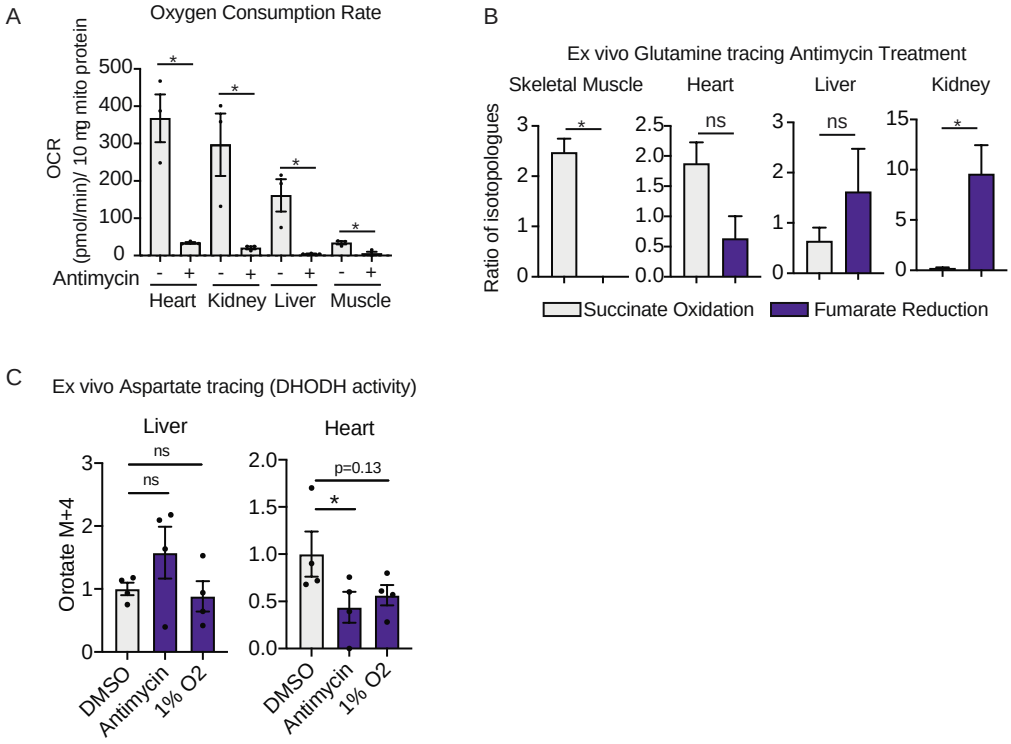

Fig. S12. Fumarate reduction supports maintenance of the mitochondrial membrane potential and nucleotide synthesis in tissues capable of net-reversal of SDH.

A. O_2 consumption rate (OCR) by mitochondria (10 μg protein) isolated from indicated tissues and treated with DMSO or 2 μM antimycin (mean +/- SEM, N=3 per condition). * indicates $P < 0.05$. P values were calculated using an unpaired parametric t test **B.** Fumarate reduction and succinate oxidation as measured by $^{13}C_5{}^{15}N_2$-glutamaine tracing for 16 hours in indicated tissues treated with 2 μM antimycin. * indicates $P < 0.05$. P values were calculated using an unpaired parametric t test **C.** *Ex vivo* 3 mM $^{13}C_4$-aspartate stable isotope tracing for 16 hours in indicated tissues kept in an incubator at 21% or 1% O_2, or treated with 2 μM antimycin in 21% O_2. Orotate M+4 levels reflect DHODH activity (mean +/- SEM, N=4 per condition). * indicates $P < 0.05$. P values were calculated using a two way ANOVA.

References and Notes

1. N. S. Chandel, D. S. McClintock, C. E. Feliciano, T. M. Wood, J. A. Melendez, A. M. Rodriguez, P. T. Schumacker, Reactive oxygen species generated at mitochondrial complex III stabilize hypoxia-inducible factor-1alpha during hypoxia: A mechanism of O2 sensing. *J. Biol. Chem.* **275**, 25130–25138 (2000). doi:10.1074/jbc.M001914200 Medline

2. D. V. Titov, V. Cracan, R. P. Goodman, J. Peng, Z. Grabarek, V. K. Mootha, Complementation of mitochondrial electron transport chain by manipulation of the NAD^+/NADH ratio. *Science* **352**, 231–235 (2016). doi:10.1126/science.aad4017 Medline

3. T. Nakagawa, S. Shimizu, T. Watanabe, O. Yamaguchi, K. Otsu, H. Yamagata, H. Inohara, T. Kubo, Y. Tsujimoto, Cyclophilin D-dependent mitochondrial permeability transition regulates some necrotic but not apoptotic cell death. *Nature* **434**, 652–658 (2005). doi:10.1038/nature03317 Medline

4. J. B. Spinelli, M. C. Haigis, The multifaceted contributions of mitochondria to cellular metabolism. *Nat. Cell Biol.* **20**, 745–754 (2018). doi:10.1038/s41556-018-0124-1 Medline

5. H. Zhang, K. J. Menzies, J. Auwerx, The role of mitochondria in stem cell fate and aging. *Development* **145**, dev143420 (2018). doi:10.1242/dev.143420 Medline

6. E. Mick, D. V. Titov, O. S. Skinner, R. Sharma, A. A. Jourdain, V. K. Mootha, Distinct mitochondrial defects trigger the integrated stress response depending on the metabolic state of the cell. *eLife* **9**, e49178 (2020). Medline

7. K. J. Condon, J. M. Orozco, C. H. Adelmann, J. B. Spinelli, P. W. van der Helm, J. M. Roberts, T. Kunchok, D. M. Sabatini, Genome-wide CRISPR screens reveal multitiered mechanisms through which mTORC1 senses mitochondrial dysfunction. *Proc. Natl. Acad. Sci. U.S.A.* **118**, e2022120118 (2021). doi:10.1073/pnas.2022120118 Medline

8. T. Ast, V. K. Mootha, Oxygen and mammalian cell culture: Are we repeating the experiment of Dr. Ox? *Nat. Metab.* **1**, 858–860 (2019). doi:10.1038/s42255-019-0105-0 Medline

9. A. J. Peacock, ABC of oxygen: Oxygen at high altitude. *BMJ* **317**, 1063–1066 (1998). doi:10.1136/bmj.317.7165.1063 Medline

10. M. C. Simon, B. Keith, The role of oxygen availability in embryonic development and stem cell function. *Nat. Rev. Mol. Cell Biol.* **9**, 285–296 (2008). doi:10.1038/nrm2354 Medline

11. L. Zheng, C. J. Kelly, S. P. Colgan, Physiologic hypoxia and oxygen homeostasis in the healthy intestine. A Review in the Theme: Cellular Responses to Hypoxia. *Am. J. Physiol. Cell Physiol.* **309**, C350–C360 (2015). doi:10.1152/ajpcell.00191.2015 Medline

12. G. L. Semenza, Targeting HIF-1 for cancer therapy. *Nat. Rev. Cancer* **3**, 721–732 (2003). doi:10.1038/nrc1187 Medline

13. B. Keith, M. C. Simon, Hypoxia-inducible factors, stem cells, and cancer. *Cell* **129**, 465–472 (2007). doi:10.1016/j.cell.2007.04.019 Medline

14. T. Kalogeris, C. P. Baines, M. Krenz, R. J. Korthuis, Cell biology of ischemia/reperfusion injury. *Int. Rev. Cell Mol. Biol.* **298**, 229–317 (2012). doi:10.1016/B978-0-12-394309-5.00006-7 Medline

15. F. Palm, Intrarenal oxygen in diabetes and a possible link to diabetic nephropathy. *Clin. Exp. Pharmacol. Physiol.* **33**, 997–1001 (2006). doi:10.1111/j.1440-1681.2006.04473.x Medline

16. H. K. Eltzschig, P. Carmeliet, Hypoxia and inflammation. *N. Engl. J. Med.* **364**, 656–665 (2011). doi:10.1056/NEJMra0910283 Medline

17. S. Vyas, E. Zaganjor, M. C. Haigis, Mitochondria and Cancer. *Cell* **166**, 555–566 (2016). doi:10.1016/j.cell.2016.07.002 Medline

18. I. Martínez-Reyes, L. R. Cardona, H. Kong, K. Vasan, G. S. McElroy, M. Werner, H. Kihshen, C. R. Reczek, S. E. Weinberg, P. Gao, E. M. Steinert, R. Piseaux, G. R. S. Budinger, N. S. Chandel, Mitochondrial ubiquinol oxidation is necessary for tumour growth. *Nature* **585**, 288–292 (2020). doi:10.1038/s41586-020-2475-6 Medline

19. R. Dumollard, M. Duchen, J. Carroll, "The role of mitochondrial function in the oocyte and embryo" in *The Mitochondrion in the Germline and Early Development*, J. C. St. John, Ed. (Academic Press, 2007), vol. 77, pp. 21–49.

20. J. Nunnari, A. Suomalainen, Mitochondria: In sickness and in health. *Cell* **148**, 1145–1159 (2012). doi:10.1016/j.cell.2012.02.035 Medline

21. M. Bajzikova, J. Kovarova, A. R. Coelho, S. Boukalova, S. Oh, K. Rohlenova, D. Svec, S. Hubackova, B. Endaya, K. Judasova, A. Bezawork-Geleta, K. Kluckova, L. Chatre, R. Zobalova, A. Novakova, K. Vanova, Z. Ezrova, G. J. Maghzal, S. Magalhaes Novais, M. Olsinova, L. Krobova, Y. J. An, E. Davidova, Z. Nahacka, M. Sobol, T. Cunha-Oliveira, C. Sandoval-Acuña, H. Strnad, T. Zhang, T. Huynh, T. L. Serafim, P. Hozak, V. A. Sardao, W. J. H. Koopman, M. Ricchetti, P. J. Oliveira, F. Kolar, M. Kubista, J. Truksa, K. Dvorakova-Hortova, K. Pacak, R. Gurlich, R. Stocker, Y. Zhou, M. V. Berridge, S. Park, L. Dong, J. Rohlena, J. Neuzil, Reactivation of Dihydroorotate Dehydrogenase-Driven Pyrimidine Biosynthesis Restores Tumor Growth of Respiration-Deficient Cancer Cells. *Cell Metab.* **29**, 399–416.e10 (2019). doi:10.1016/j.cmet.2018.10.014 Medline

22. E. Ansó, S. E. Weinberg, L. P. Diebold, B. J. Thompson, S. Malinge, P. T. Schumacker, X. Liu, Y. Zhang, Z. Shao, M. Steadman, K. M. Marsh, J. Xu, J. D. Crispino, N. S. Chandel, The mitochondrial respiratory chain is essential for haematopoietic stem cell function. *Nat. Cell Biol.* **19**, 614–625 (2017). doi:10.1038/ncb3529 Medline

23. J. Garcia-Bermudez, L. Baudrier, K. La, X. G. Zhu, J. Fidelin, V. O. Sviderskiy, T. Papagiannakopoulos, H. Molina, M. Snuderl, C. A. Lewis, R. L. Possemato, K. Birsoy, Aspartate is a limiting metabolite for cancer cell proliferation under hypoxia and in tumours. *Nat. Cell Biol.* **20**, 775–781 (2018). doi:10.1038/s41556-018-0118-z Medline

24. L. B. Sullivan, A. Luengo, L. V. Danai, L. N. Bush, F. F. Diehl, A. M. Hosios, A. N. Lau, S. Elmiligy, S. Malstrom, C. A. Lewis, M. G. Vander Heiden, Aspartate is an endogenous metabolic limitation for tumour growth. *Nat. Cell Biol.* **20**, 782–788 (2018). doi:10.1038/s41556-018-0125-0 Medline

25. S. Cardaci, L. Zheng, G. MacKay, N. J. F. van den Broek, E. D. MacKenzie, C. Nixon, D. Stevenson, S. Tumanov, V. Bulusu, J. J. Kamphorst, A. Vazquez, S. Fleming, F. Schiavi, G. Kalna, K. Blyth, D. Strathdee, E. Gottlieb, Pyruvate carboxylation enables growth of SDH-deficient cells by supporting aspartate biosynthesis. *Nat. Cell Biol.* **17**, 1317–1326 (2015). doi:10.1038/ncb3233 Medline

26. D. F. Wilson, W. L. Rumsey, T. J. Green, J. M. Vanderkooi, The oxygen dependence of mitochondrial oxidative phosphorylation measured by a new optical method for measuring oxygen concentration. *J. Biol. Chem.* **263**, 2712–2718 (1988). doi:10.1016/S0021-9258(18)69126-4 Medline

27. R. Fukuda, H. Zhang, J. W. Kim, L. Shimoda, C. V. Dang, G. L. Semenza, HIF-1 regulates cytochrome oxidase subunits to optimize efficiency of respiration in hypoxic cells. *Cell* **129**, 111–122 (2007). doi:10.1016/j.cell.2007.01.047 Medline

28. P. Lee, N. S. Chandel, M. C. Simon, Cellular adaptation to hypoxia through hypoxia inducible factors and beyond. *Nat. Rev. Mol. Cell Biol.* **21**, 268–283 (2020). doi:10.1038/s41580-020-0227-y Medline

29. M. Spinazzi, A. Casarin, V. Pertegato, L. Salviati, C. Angelini, Assessment of mitochondrial respiratory chain enzymatic activities on tissues and cultured cells. *Nat. Protoc.* **7**, 1235–1246 (2012). doi:10.1038/nprot.2012.058 Medline

30. I. H. Jain, S. E. Calvo, A. L. Markhard, O. S. Skinner, T.-L. To, T. Ast, V. K. Mootha, Genetic Screen for Cell Fitness in High or Low Oxygen Highlights Mitochondrial and Lipid Metabolism. *Cell* **181**, 716–727.e11 (2020). doi:10.1016/j.cell.2020.03.029 Medline

31. D. Tello, E. Balsa, B. Acosta-Iborra, E. Fuertes-Yebra, A. Elorza, Á. Ordóñez, M. Corral-Escariz, I. Soro, E. López-Bernardo, E. Perales-Clemente, A. Martínez-Ruiz, J. A. Enríquez, J. Aragonés, S. Cadenas, M. O. Landázuri, Induction of the mitochondrial NDUFA4L2 protein by HIF-1α decreases oxygen consumption by inhibiting Complex I activity. *Cell Metab.* **14**, 768–779 (2011). doi:10.1016/j.cmet.2011.10.008 Medline

32. S. Y. Chan, Y.-Y. Zhang, C. Hemann, C. E. Mahoney, J. L. Zweier, J. Loscalzo, MicroRNA-210 controls mitochondrial metabolism during hypoxia by repressing the iron-sulfur cluster assembly proteins ISCU1/2. *Cell Metab.* **10**, 273–284 (2009). doi:10.1016/j.cmet.2009.08.015 Medline

33. M. T. Frost, Q. Wang, S. Moncada, M. Singer, Hypoxia accelerates nitric oxide-dependent inhibition of mitochondrial complex I in activated macrophages. *Am. J. Physiol. Regul. Integr. Comp. Physiol.* **288**, R394–R400 (2005). doi:10.1152/ajpregu.00504.2004 Medline

34. I. H. Jain, L. Zazzeron, R. Goli, K. Alexa, S. Schatzman-Bone, H. Dhillon, O. Goldberger, J. Peng, O. Shalem, N. E. Sanjana, F. Zhang, W. Goessling, W. M. Zapol, V. K. Mootha, Hypoxia as a therapy for mitochondrial disease. *Science* **352**, 54–61 (2016). doi:10.1126/science.aad9642 Medline

35. P. C. Hinkle, R. A. Butow, E. Racker, B. Chance, Partial resolution of the enzymes catalyzing oxidative phosphorylation. XV. Reverse electron transfer in the flavin-

cytochrome beta region of the respiratory chain of beef heart submitochondrial particles. *J. Biol. Chem.* **242**, 5169–5173 (1967). doi:10.1016/S0021-9258(18)99410-X Medline

36. E. L. Robb, A. R. Hall, T. A. Prime, S. Eaton, M. Szibor, C. Viscomi, A. M. James, M. P. Murphy, Control of mitochondrial superoxide production by reverse electron transport at complex I. *J. Biol. Chem.* **293**, 9869–9879 (2018). doi:10.1074/jbc.RA118.003647 Medline

37. G. M. Aloysius, A. G. M. Tielens, J. J. Van Hellemond, The electron transport chain in anaerobically functioning eukaryotes. *Biochim. Biophys. Acta Bioenerg.* **1365**, 71–78 (1998). doi:10.1016/S0005-2728(98)00045-0

38. A. R. Mullen, W. W. Wheaton, E. S. Jin, P.-H. Chen, L. B. Sullivan, T. Cheng, Y. Yang, W. M. Linehan, N. S. Chandel, R. J. DeBerardinis, Reductive carboxylation supports growth in tumour cells with defective mitochondria. *Nature* **481**, 385–388 (2011). doi:10.1038/nature10642 Medline

39. C. M. Metallo, P. A. Gameiro, E. L. Bell, K. R. Mattaini, J. Yang, K. Hiller, C. M. Jewell, Z. R. Johnson, D. J. Irvine, L. Guarente, J. K. Kelleher, M. G. Vander Heiden, O. Iliopoulos, G. Stephanopoulos, Reductive glutamine metabolism by IDH1 mediates lipogenesis under hypoxia. *Nature* **481**, 380–384 (2011). doi:10.1038/nature10602 Medline

40. E. T. Chouchani, V. R. Pell, E. Gaude, D. Aksentijević, S. Y. Sundier, E. L. Robb, A. Logan, S. M. Nadtochiy, E. N. J. Ord, A. C. Smith, F. Eyassu, R. Shirley, C.-H. Hu, A. J. Dare, A. M. James, S. Rogatti, R. C. Hartley, S. Eaton, A. S. H. Costa, P. S. Brookes, S. M. Davidson, M. R. Duchen, K. Saeb-Parsy, M. J. Shattock, A. J. Robinson, L. M. Work, C. Frezza, T. Krieg, M. P. Murphy, Ischaemic accumulation of succinate controls reperfusion injury through mitochondrial ROS. *Nature* **515**, 431–435 (2014). doi:10.1038/nature13909 Medline

41. A. Reddy, L. H. M. Bozi, O. K. Yaghi, E. L. Mills, H. Xiao, H. E. Nicholson, M. Paschini, J. A. Paulo, R. Garrity, D. Laznik-Bogoslavski, J. C. B. Ferreira, C. S. Carl, K. A. Sjøberg, J. F. P. Wojtaszewski, J. F. Jeppesen, B. Kiens, S. P. Gygi, E. A. Richter, D. Mathis, E. T. Chouchani, pH-Gated Succinate Secretion Regulates Muscle Remodeling in Response to Exercise. *Cell* **183**, 62–75.e17 (2020). doi:10.1016/j.cell.2020.08.039 Medline

42. C. Chinopoulos, Succinate in ischemia: Where does it come from? *Int. J. Biochem. Cell Biol.* **115**, 105580 (2019). doi:10.1016/j.biocel.2019.105580 Medline

43. J. Zhang, Y. T. Wang, J. H. Miller, M. M. Day, J. C. Munger, P. S. Brookes, Accumulation of Succinate in Cardiac Ischemia Primarily Occurs via Canonical Krebs Cycle Activity. *Cell Rep.* **23**, 2617–2628 (2018). doi:10.1016/j.celrep.2018.04.104 Medline

44. A. R. Mullen, Z. Hu, X. Shi, L. Jiang, L. K. Boroughs, Z. Kovacs, R. Boriack, D. Rakheja, L. B. Sullivan, W. M. Linehan, N. S. Chandel, R. J. DeBerardinis, Oxidation of alpha-ketoglutarate is required for reductive carboxylation in cancer cells with mitochondrial defects. *Cell Rep.* **7**, 1679–1690 (2014). doi:10.1016/j.celrep.2014.04.037 Medline

45. C. M. Bisbach, D. T. Hass, B. M. Robbings, A. M. Rountree, M. Sadilek, I. R. Sweet, J. B. Hurley, Succinate Can Shuttle Reducing Power from the Hypoxic Retina to the O_2-Rich Pigment Epithelium. *Cell Rep.* **31**, 107606 (2020). doi:10.1016/j.celrep.2020.107606 Medline

46. H. R. Pershad, J. Hirst, B. Cochran, B. A. C. Ackrell, F. A. Armstrong, Voltammetric studies of bidirectional catalytic electron transport in Escherichia coli succinate dehydrogenase: Comparison with the enzyme from beef heart mitochondria. *Biochim. Biophys. Acta* **1412**, 262–272 (1999). doi:10.1016/S0005-2728(99)00066-3 Medline

47. A. Guarás, E. Perales-Clemente, E. Calvo, R. Acín-Pérez, M. Loureiro-Lopez, C. Pujol, I. Martínez-Carrascoso, E. Nuñez, F. García-Marqués, M. A. Rodríguez-Hernández, A. Cortés, F. Diaz, A. Pérez-Martos, C. T. Moraes, P. Fernández-Silva, A. Trifunovic, P. Navas, J. Vazquez, J. A. Enríquez, The CoQH2/CoQ Ratio Serves as a Sensor of Respiratory Chain Efficiency. *Cell Rep.* **15**, 197–209 (2016). doi:10.1016/j.celrep.2016.03.009 Medline

48. E. Perales-Clemente, M. P. Bayona-Bafaluy, A. Pérez-Martos, A. Barrientos, P. Fernández-Silva, J. A. Enriquez, Restoration of electron transport without proton pumping in mammalian mitochondria. *Proc. Natl. Acad. Sci. U.S.A.* **105**, 18735–18739 (2008). doi:10.1073/pnas.0810518105 Medline

49. S. W. Perry, J. P. Norman, J. Barbieri, E. B. Brown, H. A. Gelbard, Mitochondrial membrane potential probes and the proton gradient: A practical usage guide. *Biotechniques* **50**, 98–115 (2011). doi:10.2144/000113610 Medline

50. C. Jang, L. Chen, J. D. Rabinowitz, Metabolomics and Isotope Tracing. *Cell* **173**, 822–837 (2018). doi:10.1016/j.cell.2018.03.055 Medline

51. P. W. Hochachka, R. H. Dressendorfer, Succinate accumulation in man during exercise. *Eur. J. Appl. Physiol. Occup. Physiol.* **35**, 235–242 (1976). doi:10.1007/BF00423282 Medline

52. M. P. King, G. Attardi, Human cells lacking mtDNA: Repopulation with exogenous mitochondria by complementation. *Science* **246**, 500–503 (1989). doi:10.1126/science.2814477 Medline

53. M. A. Selak, S. M. Armour, E. D. MacKenzie, H. Boulahbel, D. G. Watson, K. D. Mansfield, Y. Pan, M. C. Simon, C. B. Thompson, E. Gottlieb, Succinate links TCA cycle dysfunction to oncogenesis by inhibiting HIF-alpha prolyl hydroxylase. *Cancer Cell* **7**, 77–85 (2005). doi:10.1016/j.ccr.2004.11.022 Medline

54. A. Viale, P. Pettazzoni, C. A. Lyssiotis, H. Ying, N. Sánchez, M. Marchesini, A. Carugo, T. Green, S. Seth, V. Giuliani, M. Kost-Alimova, F. Muller, S. Colla, L. Nezi, G. Genovese, A. K. Deem, A. Kapoor, W. Yao, E. Brunetto, Y. Kang, M. Yuan, J. M. Asara, Y. A. Wang, T. P. Heffernan, A. C. Kimmelman, H. Wang, J. B. Fleming, L. C. Cantley, R. A. DePinho, G. F. Draetta, Oncogene ablation-resistant pancreatic cancer cells depend on mitochondrial function. *Nature* **514**, 628–632 (2014). doi:10.1038/nature13611 Medline

55. F. Weinberg, R. Hamanaka, W. W. Wheaton, S. Weinberg, J. Joseph, M. Lopez, B. Kalyanaraman, G. M. Mutlu, G. R. S. Budinger, N. S. Chandel, Mitochondrial metabolism and ROS generation are essential for Kras-mediated tumorigenicity. *Proc. Natl. Acad. Sci. U.S.A.* **107**, 8788–8793 (2010). doi:10.1073/pnas.1003428107 Medline

56. S. Boukalova, J. Stursa, L. Werner, Z. Ezrova, J. Cerny, A. Bezawork-Geleta, A. Pecinova, L. Dong, Z. Drahota, J. Neuzil, Mitochondrial Targeting of Metformin Enhances Its Activity against Pancreatic Cancer. *Mol. Cancer Ther.* **15**, 2875–2886 (2016). doi:10.1158/1535-7163.MCT-15-1021 Medline

57. K. K. Brown, J. B. Spinelli, J. M. Asara, A. Toker, Adaptive Reprogramming of *De Novo* Pyrimidine Synthesis Is a Metabolic Vulnerability in Triple-Negative Breast Cancer. *Cancer Discov.* **7**, 391–399 (2017). doi:10.1158/2159-8290.CD-16-0611 Medline

58. J. Rohlena, L.-F. Dong, S. J. Ralph, J. Neuzil, Anticancer drugs targeting the mitochondrial electron transport chain. *Antioxid. Redox Signal.* **15**, 2951–2974 (2011). doi:10.1089/ars.2011.3990 Medline

59. A. N. Lau, M. G. Vander Heiden, Metabolism in the Tumor Microenvironment. *Annu. Rev. Cancer Biol.* **4**, 17–40 (2020). doi:10.1146/annurev-cancerbio-030419-033333

60. P. Jha, X. Wang, J. Auwerx, Analysis of Mitochondrial Respiratory Chain Supercomplexes Using Blue Native Polyacrylamide Gel Electrophoresis (BN-PAGE). *Curr. Protoc. Mouse Biol.* **6**, 1–14 (2016). doi:10.1002/9780470942390.mo150182 Medline

61. R. Acín-Pérez, P. Fernández-Silva, M. L. Peleato, A. Pérez-Martos, J. A. Enriquez, Respiratory active mitochondrial supercomplexes. *Mol. Cell* **32**, 529–539 (2008). doi:10.1016/j.molcel.2008.10.021 Medline

62. S. W. Chan, J. Z. Chen, "Measuring mtDNA damage using a supercoiling-sensitive qPCR approach" in *Mitochondrial DNA: Methods and Protocols*, J. A. Stuart, Ed. (Humana, 2009), pp. 183–197.

63. N. Burger, A. Logan, T. A. Prime, A. Mottahedin, S. T. Caldwell, T. Krieg, R. C. Hartley, A. M. James, M. P. Murphy, A sensitive mass spectrometric assay for mitochondrial CoQ pool redox state in vivo. *Free Radic. Biol. Med.* **147**, 37–47 (2020). doi:10.1016/j.freeradbiomed.2019.11.028 Medline

64. P. Heinrich, C. Kohler, L. Ellmann, P. Kuerner, R. Spang, P. J. Oefner, K. Dettmer, Correcting for natural isotope abundance and tracer impurity in MS-, MS/MS- and high-resolution-multiple-tracer-data from stable isotope labeling experiments with IsoCorrectoR. *Sci. Rep.* **8**, 17910 (2018). doi:10.1038/s41598-018-36293-4 Medline